

# 1 **Linking plasmid-based beta-lactamases to their bacterial hosts using single-cell fusion PCR**

2

3 Peter J. Diebold<sup>1</sup>, Felicia N. New<sup>1</sup>, Michael Hovan<sup>2</sup>, Michael J. Satlin<sup>3</sup>, Ilana L. Brito<sup>1\*</sup>

4 <sup>1</sup>Meinig School of Biomedical Engineering, Cornell University, Ithaca, NY

5 <sup>2</sup>Robert Wood Johnson Medical School, New Brunswick, NJ

6 <sup>3</sup>Weill Cornell Medicine, Cornell University, New York, NY

7 \* Please send all correspondences to: [ibrito@cornell.edu](mailto:ibrito@cornell.edu)

8

## 9 **Abstract**

10 The horizontal transfer of plasmid-encoded genes allows bacteria to adapt to constantly shifting  
11 environmental pressures, bestowing functional advantages to their bacterial hosts such as antibiotic  
12 resistance, metal resistance, virulence factors, and polysaccharide utilization. However, common  
13 molecular methods such as short- and long-read sequencing of microbiomes cannot associate  
14 extrachromosomal plasmids with the genome of the host bacterium. Alternative methods to link plasmids  
15 to host bacteria are either laborious, expensive or prone to contamination. Here we present the One-step  
16 Isolation and Lysis PCR (OIL-PCR) method, which molecularly links target ARGs with the bacterial 16S  
17 rRNA gene via fusion PCR performed within an emulsion. After validating this method, we apply it to  
18 identify the bacterial hosts of three clinically relevant beta-lactamases in a neutropenic patient population  
19 who are particularly vulnerable multidrug-resistant infections. We detect novel associations of two low-  
20 abundance genera, *Romboutsia* and *Agathobacter*, with a multi-drug resistant plasmid harbored by  
21 *Klebsiella pneumoniae*. We put forth a robust, accessible, and high-throughput platform for sensitively  
22 surveying the bacterial hosts of mobile genes in complex microbial communities.

## 23 **Introduction**

24 The emergence of multidrug-resistant (MDR) pathogens is a grave public health threat that occurs when  
25 pathogenic bacteria acquire antibiotic resistant genes (ARGs) through horizontal gene transfer (HGT)  
26 with bacteria in their proximal environment. The gut microbiome harbors a diverse repertoire of ARGs  
27 and these genes have been proposed to serve as a reservoir for HGT with MDR pathogens<sup>1</sup>. ARGs are  
28 often carried on mobilizable plasmids that impose technical challenges to surveying the set of bacteria  
29 affiliated with these genes. Standard molecular tools such as PCR and next-generation sequencing often  
30 fail to associate mobile ARGs with their bacterial hosts because they cannot capture the cellular context  
31 of extrachromosomal genes in the case of plasmids. Novel untargeted sequencing methods, such as  
32 bacterial Hi-C<sup>2</sup> and methylation profiling<sup>3</sup>, provide broad reconstruction of plasmid-host relationships in  
33 metagenomes, as a trade-off for sensitivity. Alternatively, single-cell whole genome sequencing offers an  
34 ideal solution to this problem, but may be lower throughput, more expensive and require specialized  
35 equipment<sup>4,5</sup>. Targeted methods, such as bacterial cell culture under antibiotic selection, require that the  
36 ARG is expressed, functional, and selective in all hosts. Applying this broadly to capture the full diversity  
37 of the gut microbiome is complicated by the need for wide-ranging media and growth conditions<sup>6,7</sup>.

38 Single-cell qPCR is a targeted method to identify the hosts of specific genes, however each use  
39 specialized microfluidic devices, are limited in bacterial taxa they can capture, and most do not allow  
40 direct sequencing of the PCR products<sup>8-10</sup>. Alternatively, epicPCR<sup>11</sup>, uses fusion PCR and two emulsion  
41 steps to associate a taxonomic marker with a functional gene. Sequencing the fused PCR products  
42 provides accurate and sensitive associations between 16S sequence taxonomy and a given target gene.  
43 However, this method can be challenging to execute, difficult to scale up for multiple samples, and  
44 utilizes toxic and difficult-to-acquire reagents.

45 Here, we put forth One-step Isolation and Lysis PCR (OIL-PCR), a method that detects host-ARG  
46 associations from complex microbial communities through cellular emulsion and fusion PCR. Our  
47 streamlined method, based on the innovation of epicPCR, simplifies the procedure by combining the two

48 emulsion steps of cell lysis and fusion PCR into a single emulsion PCR reaction that can be performed in  
49 a 96-well format using robotic automation. Furthermore, OIL-PCR can be multiplexed to target at least  
50 three genes in the same reaction, uses non-toxic commercially available reagents, and can be performed  
51 without relying on microfluidics or specialized equipment. Validation experiments on three  
52 environmental bacterial communities reveal that OIL-PCR is highly accurate and specific. We  
53 demonstrate the utility of this approach in examining the novel association of three extended spectrum  
54 beta-lactamase (ESBL) genes with two commensal organisms in the gut. Our results highlight the utility  
55 of this method in defining mobile ARG distribution within microbial communities as complex as the  
56 human gut microbiome.

## 57 **Results**

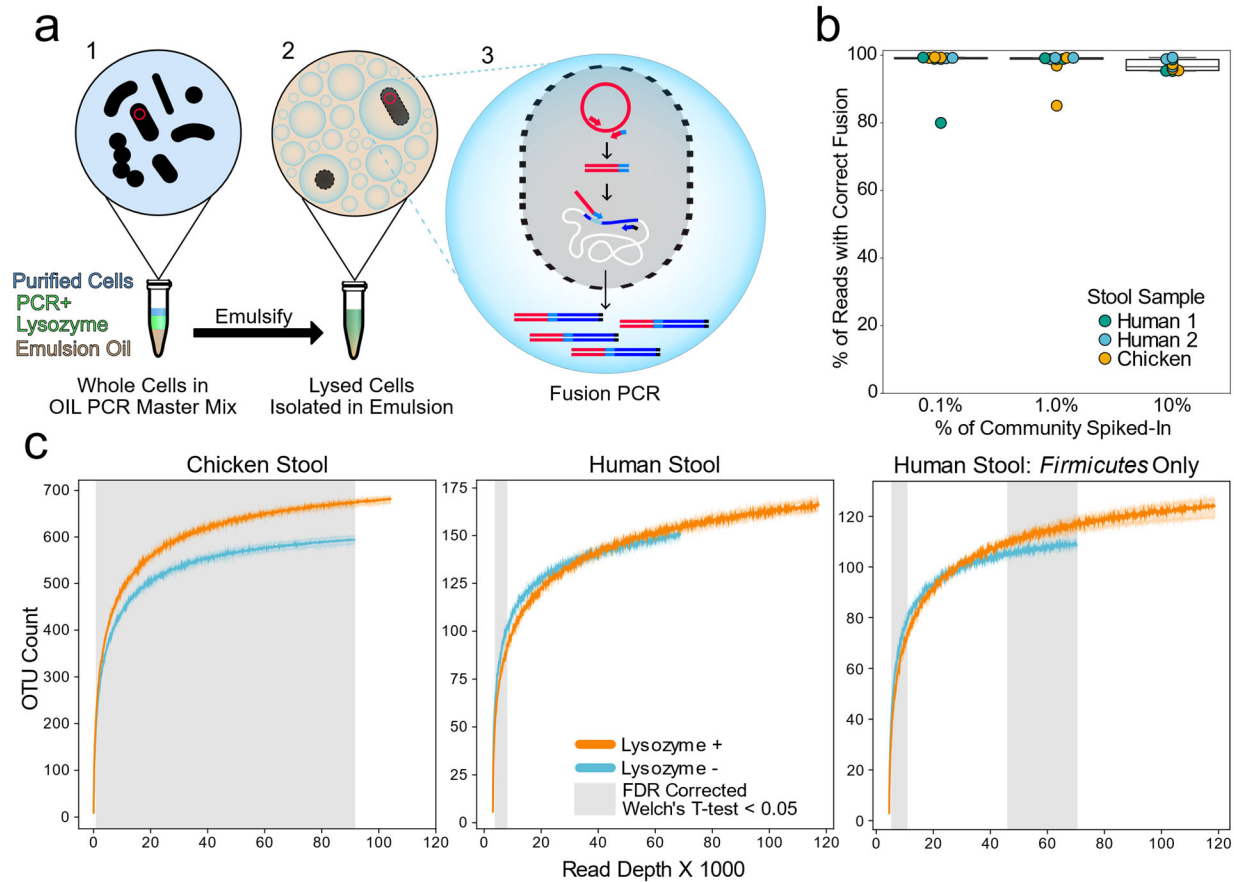
### 58 **Development of a One-step Isolation and Lysis PCR method**

59 OIL-PCR applies established fusion PCR methods to fuse any gene of interest to the 16S rRNA gene  
60 using three primers: two primers hybridize to the target gene, and a universal 16S reverse primer  
61 hybridizes to the V4 region. Amplification of the target gene appends a universal 16S forward primer  
62 sequence to the end of the target amplicon via a tailed reverse primer. The target gene amplicon then acts  
63 as a primer for amplification and hybridizes to the 16S rRNA gene as a forward primer, producing a fused  
64 gene product containing both the target gene and the 16S V4 sequence (Fig. 1a, Supplementary Fig. 1).

65 For fusion PCR to accurately link target genes with host marker genes, cells must be isolated to prevent  
66 the formation of non-specific fusion products. Oil emulsions and microwells have long been used to  
67 isolate eukaryotic cells, however, it is difficult to lyse bacteria in this format, especially gram-positive  
68 bacteria due to their thick cell walls. Existing single-cell isolation methods for bacteria either do not  
69 address this problem<sup>9,10</sup>, rely on specialized microfluidics<sup>12</sup> or use time-consuming methods to  
70 encapsulate bacteria within hydrogel beads before performing multi-step chemical and enzymatic lysis

71 procedures<sup>11,13</sup>. To address this problem, OIL-PCR combines bacterial isolation, lysis, and fusion PCR  
72 into a single streamlined reaction.

73



74 **Figure 1. OIL-PCR can specifically link plasmid-encoded genes with their hosts**

75 a) Depiction of the OIL-PCR method. (1) Nycodenz-purified cells are mixed with PCR master mix,  
76 lysozyme, and emulsion oil and shaken to create an emulsion. (2) Cells are lysed within the  
77 emulsion. (3) Fusion PCR is performed in droplets containing cells harboring the targeted gene.  
78 Fused amplicons between the gene of interest and the 16S rRNA gene are the product.  
79 b) A boxplot showing the percent of Illumina reads containing correct fusion products, namely the  
80 fusion of plasmid-borne *cmR* and the 16S rRNA gene of *E. coli* MG1655. OIL-PCR was

81 performed on two individuals' and one chicken's gut microbiome sample, spiked with varying  
82 concentrations of *E. coli*.

83 c) Rarefaction analysis of chicken (left) or human gut microbiome sample (middle) with (orange)  
84 and without (blue) lysozyme treatment. At right is the rarefaction analysis performed on  
85 Firmicutes only in the human stool sample. Grayed regions in the plot represent areas where the  
86 curves are significantly different ( $p < 0.05$ ) from one another, according to an FDR-corrected  
87 Welch's t-test.

88

89

90 We developed a protocol that allows for the incorporation of Ready-Lyse (RL) Lysozyme into the fusion  
91 PCR master mix. Whole bacterial cells are added directly to the master mix while on ice to inhibit lytic  
92 activity during sample preparation. Vigorous shaking of the mixture then encapsulates the individual cells  
93 in an emulsion. Warming the emulsion to 37 °C activates the enzyme, lysing the cells. Next, a standard  
94 PCR thermocycler carries out the fusion PCR reactions in the single-cell emulsions. Fused PCR products  
95 are purified from the emulsion and amplified further with a nested primer to filter out off-target PCR  
96 products and add Illumina adapters. Lastly, custom indexing primers are used to index the fused products  
97 before Illumina sequencing. Our experiments confirmed the compatibility of the RL Lysozyme with the  
98 fusion PCR reaction, but required the addition of bovine serum albumin, a globular protein known to  
99 reduce protein aggregation<sup>14</sup> (Supplementary Fig. 2a). We found that RL retained full activity in the  
100 standard NEB Phusion HF buffer (Supplementary Fig. 2c).

101 Next, we optimized the fusion PCR master mix to maintain a stable emulsion and amplify efficiently in  
102 picoliter droplets. PCR emulsions were prepared with fluorinated oil as used in modern emulsion-based  
103 methods, such as Drop-Seq<sup>15</sup>. We combined the fusion PCR master mix with bacterial cells and emulsion  
104 oil in either a 1.5 ml tube or a 0.5 ml deep-well plate before emulsifying the mixture using a tabletop bead

105 homogenizer. Unlike microfluidic-enabled emulsions, our protocol leverages equipment commonly found  
106 in most molecular biology laboratories. We stabilized the emulsion by using detergent-free buffers and  
107 improved the efficiency of the PCR amplification within the emulsion by adding additional polymerase,  
108 BSA, dithiothreitol (DTT), and ammonium sulfate. We found that the addition of extra MgCl<sub>2</sub> mitigated  
109 the inhibitory effects of extremely high concentrations of cell debris within droplets after lysis  
110 (Supplementary Fig. 1b).

### 111 **OIL-PCR accurately associates plasmid genes with the host in a binary community**

112 In any emulsion-based method, it is essential to optimize the concentration of input cells to prevent the  
113 encapsulation of two or more cells in the same droplet. When using a monodisperse emulsion such as  
114 those generated using microfluidics, the ideal concentration of input cells is chosen using a Poisson  
115 distribution<sup>8-10</sup>. However, these calculations are not reliable in the case of a polydisperse emulsion, as  
116 employed here. We therefore developed a probe-based TaqMan qPCR assay to experimentally verify the  
117 optimal concentration of input cells that prevented non-specific gene fusions (Supplementary Fig. 3a).  
118 OIL-PCR was performed on a binary community consisting of *E. coli* carrying the chloramphenicol  
119 resistance gene *cmR* on a plasmid and WT *V. cholerae*. The two strains were mixed 1:1 and we performed  
120 OIL-PCR with a fusion primer set specific to *cmR* and universally targeting the 16S rRNA gene<sup>11</sup>  
121 (Supplementary Table T2 and T3). A gradient of cell input concentrations was used and the final PCR  
122 products were recovered and purified. We then performed probe-based qPCR on the purified product  
123 using a nested primer for *cmR*, two blocking primers to inactivate any unfused amplicons, and two  
124 distinct fluorescent TaqMan probes (Thermo-Fisher 4316034) to specifically target the V4 region of  
125 either *E. coli* or *V. cholerae* (Supplementary Table T2). The fluorescent signal from each probe measured  
126 the relative ratio of specific to non-specific gene fusions present in the final amplicon pool  
127 (Supplementary Fig. 3a). When the input concentration of cells was at or lower than 400 cells/μl, or 40 k  
128 cells per reaction, non-specific gene fusion detection was reduced to undetectable levels (Supplementary  
129 Fig. 3b). As well as confirming that bacterial cells were isolated within the emulsion, we further

130 confirmed that droplets did not coalesce by performing the TaqMan assay on OIL-PCR products from *E.*  
131 *coli* and *V. cholerae* cells combined after they were individually emulsified (Supplementary Fig. 3b). Our  
132 results confirmed that the emulsion is highly stable and coalescence was undetected.

133 **Application of OIL-PCR to environmental microbial communities allows robust and sensitive**  
134 **association of extrachromosomal elements with their host.**

135 Using OIL-PCR on environmental microbial communities requires clean bacterial cell preparations free  
136 of environmental contaminants which may inhibit PCR. To address this concern, cells were purified using  
137 Nycodenz density gradient centrifugation<sup>16,17</sup>, a simple method that can isolate clean bacterial fractions  
138 with minimal handling time to reduce contamination. Additionally, concerned that cell-free DNA can  
139 stick to the membranes and cell walls of bacteria<sup>18</sup> thus introducing noisy associations in the data, we  
140 treated cells with heat-labile double strand-specific DNase (dsDNase). This enzyme only digests  
141 unprotected double stranded genomic DNA present in the samples without degrading single strand  
142 primers. By controlling the enzyme concentration, temperature, and speed at which cells were processed,  
143 we were able to digest extra-cellular DNA without impacting PCR efficiency of cellular contents. Using  
144 our Taqman assay, we demonstrated that including dsDNase treatment has the potential to increase the  
145 total cell input per reaction tenfold (Supplementary Fig. 3d).

146 To test the accuracy of our method on environmental samples, we spiked *Escherichia coli* MG1655<sup>19</sup>  
147 containing plasmid pBAD33<sup>20</sup> harboring *cmR* into two human and one chicken stool samples that lacked  
148 the gene according to PCR screening. Our results show that when *E. coli* was incorporated at 0.1%, or  
149 about 20 cells total, 97.8% of the reads (or 99.2%, excluding a single outlier) demonstrated the correct  
150 association when the test strain of *E. coli* was incorporated at 0.1%, or about 20 cells total, highlighting  
151 the sensitivity of OIL-PCR to detect the associations of genes in low abundant species across different  
152 sample types. The accuracy of OIL-PCR decreases slightly when the targeted sequence increases to 10%  
153 of the community composition, although associations were still 97% correct on average.

154 **Lysozyme improves capture of difficult-to-lyse gram positive bacteria**

155 To achieve our goal of robust lysis and amplification to screen all bacteria within a complex community,  
156 we measured the effect lysozyme had on bacterial detection. We performed standard 16S sequencing on  
157 human and chicken stool communities using OIL-PCR, testing three variables: the effect of lysozyme,  
158 dsDNase, and heat inactivation of dsDNase on total bacterial recovery (Supplementary Fig. 4). All eight  
159 combinations of the three variables were tested in duplicate for two stool samples using robotic  
160 automation. For our analysis, we chose to focus on the total number of operational taxonomic units  
161 (OTUs) captured in our data rather than relative abundance metrics, as this better reflects our goal of  
162 detecting species, rather than recapitulating the starting community structure.

163 First, we assayed how each of the three variables (RL, dsDNase, and heat inactivation) affected OTU  
164 recovery. Based on rarefaction curves, we found dsDNase and Heat inactivation had no significant effect  
165 on OTU recovery in human and chicken stool, while RL lysozyme significantly increase OTU recovery in  
166 chicken stool based on Welch's T-test with Benjamini-Hochberg FDR correction (Fig 1, Supplementary  
167 Fig. 4). RL was the only variable that significantly changed OTU recovery and therefore it was the only  
168 variable included in our final protocol.

169 Next, we looked to see whether any taxonomic groups were being enriched or depleted with lysozyme.  
170 Technical replicate OTU tables were combined to allow for deeper sampling depth. Results show that no  
171 phylum was significantly depleted, and importantly, at higher sequencing depths, *Firmicutes* were  
172 enriched in both the human and chicken samples. Additionally, *Bacteroides* species were enriched in the  
173 chicken sample. These results demonstrate the benefit of RL Lysozyme for capturing difficult to lyse  
174 gram-positive bacteria in the Firmicutes phylum, which account for much of the commensal diversity  
175 within the gut microbiome

176 We noticed that the total number of OTUs recovered from OIL-PCR was significantly lower than 16S  
177 sequencing of the input community at the same sampling depth (Supplementary Fig. 5). We hypothesized



178 the reason for this dramatic reduction in OTUs was due to subsampling bias introduced through low cell  
179 input and variable amplification efficiency in OIL-PCR. To test our hypothesis, we combined OTU tables  
180 from two, four and eight technical replicates and found a consistent up-shift for each rarefaction curve as  
181 we combined more tables. This up-shift was not observed when combining the input Nycodenz  
182 sequencing, indicating that the reduced OTU counts were due in part to sub-sampling bias and not an  
183 inherent failure to capture bacterial taxa (Supplemental Fig. 5). We therefore recommend OIL-PCR to be  
184 performed in replicates such that a sufficient number of cells are being sampled.

### 185 **Increased throughput through automation and multiplexing**

186 To further improve the efficiency and throughput of OIL-PCR, we sought to transition the method from  
187 1.5 ml centrifuge tubes to a 96-well plate format using the Eppendorf epMotion liquid handling robot.  
188 The liquid handling robot can perform certain parts of the PCR preparation as well as DNA recovery and  
189 purification. The automated workflow allowed us to process up to 48 samples simultaneously with fewer  
190 manual steps overall.

191 We next tested whether OIL-PCR could simultaneously target multiple genes through multiplexing. We  
192 repeated the previously described TaqMan assay using a strain of *V. cholerae* containing the ampicillin  
193 resistance gene *ampR* and *E. coli* with *cmR*; both on a plasmid (Supplementary Fig. 3c). Our results  
194 demonstrate that OIL-PCR can be multiplexed while still accurately maintaining the correct associations  
195 of target genes with their host bacteria.

### 196 **Bacterial hosts are identified for several clinically important $\beta$ -lactamase genes**

197 We analyzed metagenomic sequencing of stool samples that were collected from a cohort of patients who  
198 were neutropenic because of chemotherapy administered for a hematopoietic cell transplant. Two  
199 patients, B335 and B314, were chosen for OIL-PCR based on the presence of three class-A beta-  
200 lactamase genes, *bla<sub>TEM</sub>*, *bla<sub>SHV</sub>*, and *bla<sub>CTX-M</sub>* in the metagenomes. We tested a three-sample time course  
201 from patient B335: before antibiotic treatment, after four days of trimethoprim-sulfamethoxazole and one

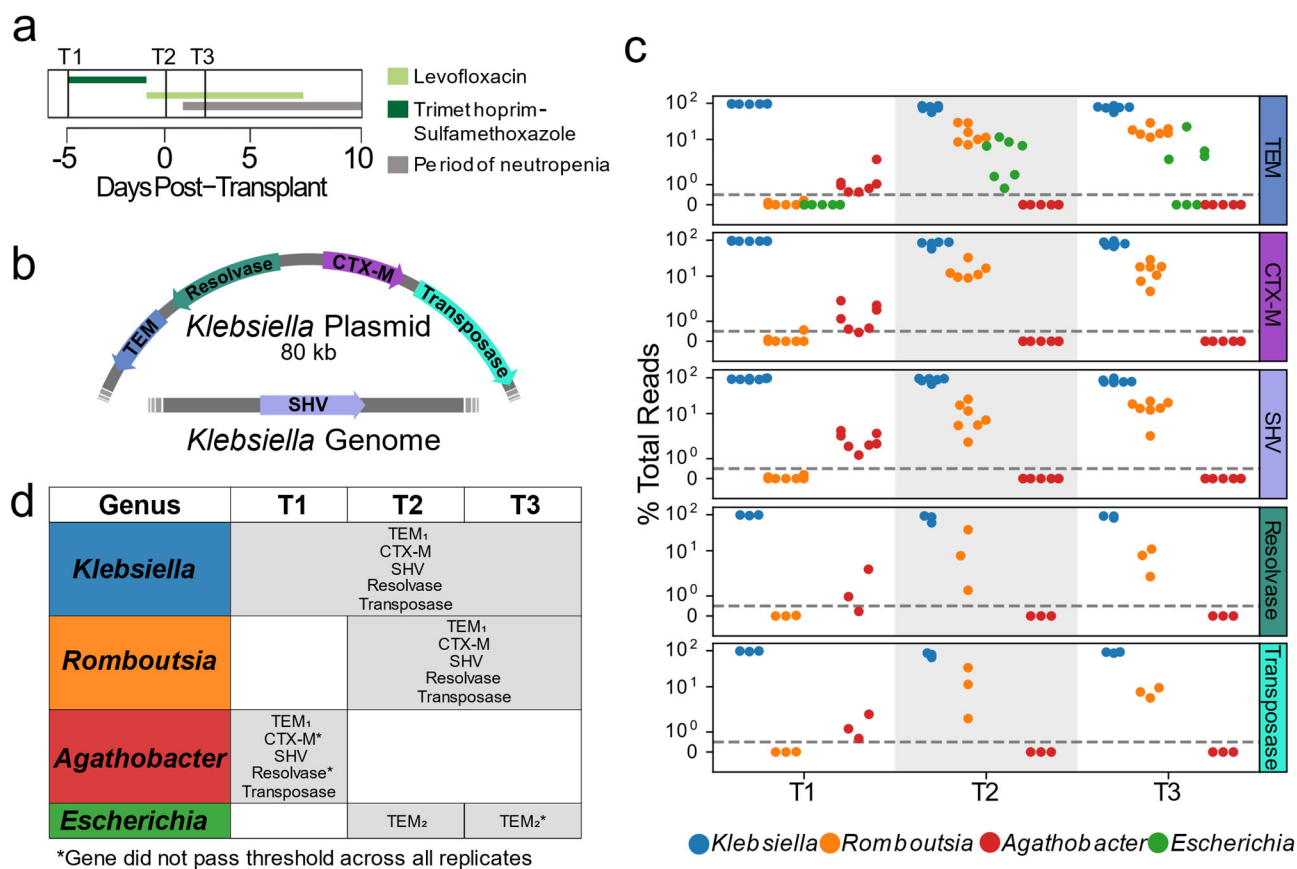
202 day of levofloxin, and lastly after an additional two days of levofloxin (Fig. 2a). Patient B335 carried all  
203 three genes across three time points with *bla<sub>TEM</sub>* and *bla<sub>CTX-M</sub>* on an 80 kb *Klebsiella* plasmid and *bla<sub>SHV</sub>*  
204 on a contig that was annotated as *Klebsiella* (Fig. 2b). We tested one sample from patient B314 from  
205 before antibiotic treatment which carried multiple *bla<sub>SHV</sub>* genes (Supplementary Fig. 6). We hypothesized  
206 that OIL-PCR could be used to sensitively and accurately detect additional hosts of these genes.

207 We designed three degenerate fusion primer sets to broadly target most variants of *bla<sub>TEM</sub>*, *bla<sub>SHV</sub>*, and  
208 *bla<sub>CTX-M</sub>* (Supplementary Table T2, T3), and performed multiplexed OIL-PCR with robotic automation.  
209 Samples were processed in quadruplicates along with negative and positive controls. We set a threshold  
210 for defining positive gene-taxa associations, as having 0.5% of total reads across the four replicates.

211 Our OIL-PCR results largely confirm findings in the metagenomic assemblies from Kent et al.<sup>2</sup>. In B314,  
212 we found *bla<sub>SHV</sub>* associated with *Klebsiella* as suggested by metagenomic assemblies. However, we also  
213 detected two other class-A beta-lactamase genes, *bla<sub>LEN</sub>* and *bla<sub>OXY</sub>*, which were present in the  
214 metagenomes but we did not expect to amplify with our primers. *bla<sub>LEN</sub>* amplified with the primers  
215 designed for *bla<sub>SHV</sub>* and *bla<sub>OXY</sub>* amplified with primers for *bla<sub>CTX-M</sub>*. Curiously, *bla<sub>OXY</sub>* is an exceptionally  
216 poor match for our *bla<sub>CTX-M</sub>* primers, having a mismatch one base away from the 5' end of the fusion  
217 primer. We hypothesize that the low annealing temperature and modified buffer used in the emulsion  
218 PCR is highly permissive to priming mismatches. We see permissive annealing as an advantage for the  
219 method because it allows for amplification of unknown variants of target genes while amplification due to  
220 off-target priming is filtered out during the nested PCR step (Supplementary Fig. 1), leaving only the true  
221 amplicons in the final sequencing. This permissive annealing behavior of OIL-PCR can be leveraged in  
222 the future to design broad-range primers for diverse gene groups such as metallo-beta-lactamases<sup>24</sup>.

223 Results from patient B335's time course also matched the metagenomic sequencing from Kent et al.,  
224 associating *bla<sub>TEM</sub>*, *bla<sub>SHV</sub>*, and *bla<sub>CTX-M</sub>* with *Klebsiella* in all three time points (Fig. 2c,d). We also found  
225 that all three genes strongly associated with the commensal genus *Romboutsia* in time points T2 and T3  
226 and to a lesser extent with *Agathobacter* in time point T1 (Fig. 2c,d). A strain of *Escherichia* with a

227 distinct variant of *bla*<sub>TEM</sub> was detected at time point T2, but did not pass the detection threshold across all  
 228 replicates in timepoint T3. We repeated OIL-PCR on all three samples from B335, this time in triplicate  
 229 without multiplexing to further confirm these results. The singleplex experiment perfectly mirrored the  
 230 multiplex results, excluding one replicate of T2/CTX-M which failed to sequence, indicating that these  
 231 genes are linked with organisms other than *Klebsiella*. As further confirmation of this result, we targeted  
 232 two Tn3-like transposon genes situated in close proximity to *bla*<sub>TEM</sub> and *bla*<sub>CTX-M</sub> on the 80 kb *Klebsiella*  
 233 plasmid. We hypothesized that these genes should also be associated with the same genera as the ARGs.  
 234 Remarkably we observed the identical pattern with *Klebsiella*, *Romboutsia*, and *Agathobacter* as with the  
 235 three beta-lactamases, but not *Escherichia*, which carried a distinct variant of *bla*<sub>TEM</sub> (Fig 2c,d).



236 **Figure 2. Extended spectrum beta-lactamase genes are associated with both pathogenic and**  
 237 **commensal species**

238 a) Summary of treatment and sample time points for patient B335

- 239 b) Depiction of an 80kb plasmid carried by *K. pneumoniae* harboring the *bla<sub>CTX-M</sub>*, *bla<sub>TEM</sub>*, Tn3  
240 transposase and resolvase genes. The *bla<sub>SHV</sub>* gene is presumed to be carried within the *K.*  
241 *pneumoniae* genome. Placement of these genes was inferred from metagenomic assemblies of  
242 patient B335's gut microbiome sample.
- 243 c) OIL-PCR results for each of the genes depicted in (a) patient B335 at 3 time points. For all gene-  
244 taxa associations, the percent of total OIL-PCR reads for that gene-time point is plotted. All  
245 species passing our detection threshold of 0.5% (dotted line) at any of the three time points is  
246 included in this plot.
- 247 d) A table summarizing the results in (b). All gene-taxa associations for each time point passing our  
248 detection thresholds are listed. Two SNP variants of TEM were detected and denoted with  
249 subscript numbering. Gene-taxa associations which did not consistently pass our detection  
250 threshold across all replicates are noted (\*).

251

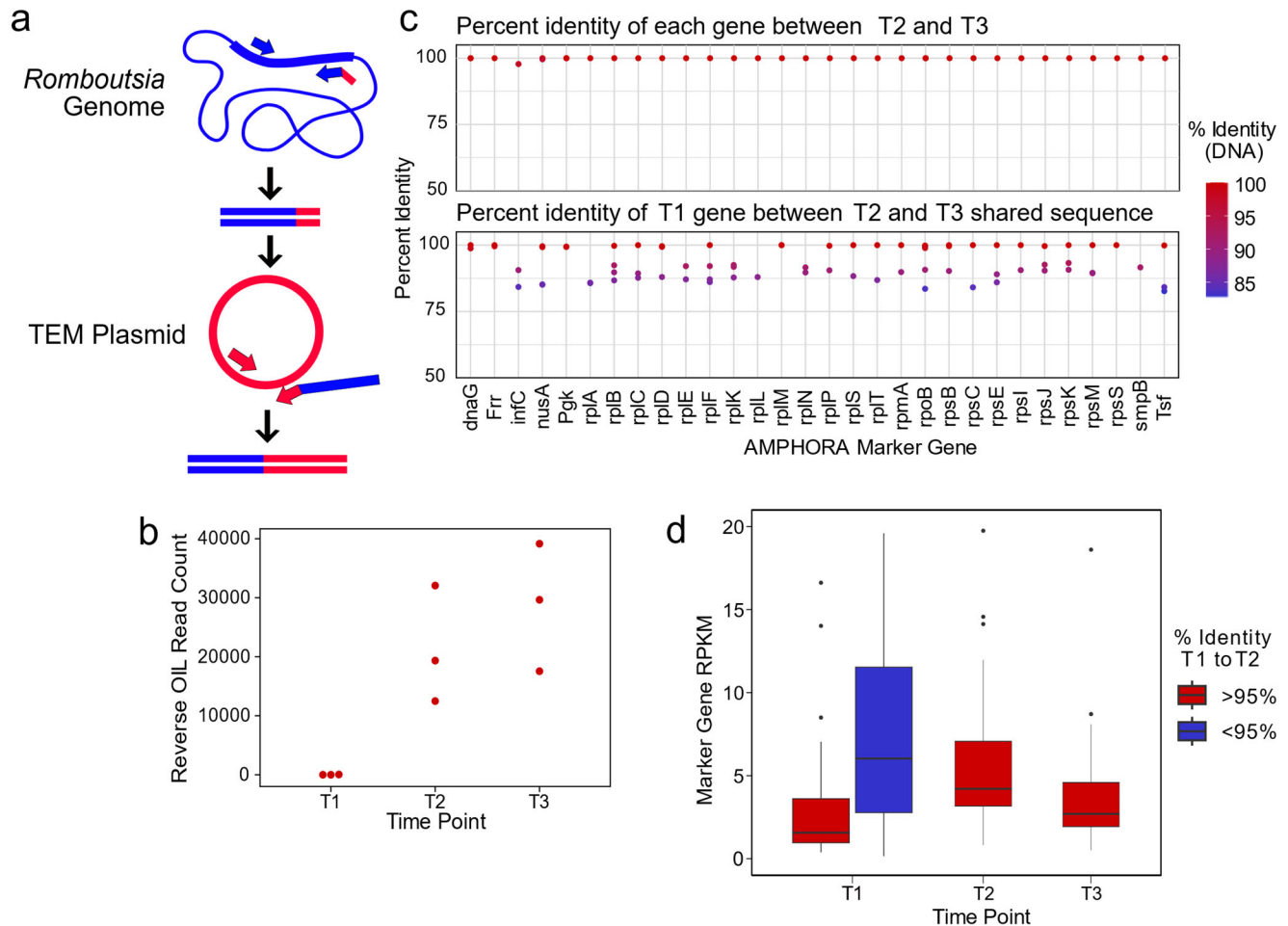
252

### 253 **OIL-PCR provides further evidence of the association of beta-lactamases with the commensal**

#### 254 ***Romboutsia***

255 We next investigated whether OIL-PCR could be used to further confirm the association between  
256 *Romboutsia* and the three beta-lactamases. We focused specifically on *Romboutsia* because of the strong  
257 signal in the OIL-PCR results compared to *Agathobacter*. For this experiment, instead of fusing the ARG  
258 sequence to the 16S rRNA gene using universal primers, we used primers designed to specifically detect  
259 the *Romboutsia* 16S rRNA<sup>25</sup> and fused the 16S gene specifically to *bla<sub>TEM</sub>* (Fig. 3a, Supplementary Table  
260 T2, T3). In this instance, no amplification is possible unless *Romboutsia* is encased in the same droplet  
261 with the *bla<sub>TEM</sub>* gene and would negate the possibility of false-positive associations due to chimera  
262 formation. Results show amplification and sequencing was only produced from time points T2 and T3

263 with no signal detected at time T1, confirming the presence of *bla*<sub>TEM</sub> within *Romboutsia* at time points T2  
 264 and T3 but not T1 (Fig. 3b).  
 265



266 **Figure 3. *R. timonensis* strains associated with the three beta-lactamase genes appear over the**  
 267 **patient's time course**

268 a) Depiction of the reverse OIL-PCR reaction in which *Romboutsia*-specific 16S rRNA sequences  
 269 (blue) are fused with the *bla*<sub>TEM</sub> sequences (red).  
 270 b) OIL-PCR read counts of the reaction shown in (a) are plotted.

- 271 c) The percent sequence identity of assembled *R. timonensis* marker genes between genes identified  
272 in timepoints 2 and 3 (top) and between timepoints 1 and between sequences shared at timepoints  
273 2 and 3 (bottom).
- 274 d) RPKM-normalized abundance-values for the assembled marker genes for each strain assembled  
275 in time point 1 and the major strain present in timepoints 2 and 3.

276  
277

278 We next explored the metagenomic data for clues as to whether the *Romboutsia* strain was present at  
279 timepoint T1, but below the detection threshold, or whether the strain linked with the genes was acquired  
280 sometime between time T1 and T2. Based on the 16S data from OIL-PCR and metagenomic sequencing,  
281 we identified the *Romboutsia* species as *R. timonensis*. Genus-level abundance data showed *R. timonensis*  
282 to be present in all three timepoints in patient B335. Due to the overall low abundance of this organism,  
283 we were unable to assemble a *Romboutsia* genome from these samples. Instead, we aligned patient  
284 B335's three samples to the *R. timonensis* (PRJEB14233) genome from NCBI, assembled the aligned  
285 reads and examined similarities between the *R. timonensis* taxonomic markers over the three timepoints  
286 (Figure 3c). We found that B335 was colonized by at least two independent strains of *R. timonensis*  
287 during the first timepoint, but that only one *R. timonensis* strain persisted during timepoint T2 and T3.  
288 One of the *R. timonensis* strains from T1 was identical to the strain from T2 and T3 across 15/30  
289 AMPHORA marker genes, and >99% identical in 24/30 genes (Fig. 3c), suggesting that the strain of *R.*  
290 *timonensis* from time T2 and T3 was also present at time point T1. We found no significant difference in  
291 the normalized abundance of *Romboutsia* between time point T1 and time points T2 and T3 (Fig. 3d),  
292 albeit our data suggests that the persistent strain is the minor variant at time point 1. Despite the  
293 sensitivity of OIL-PCR, which can detect cells at least 0.1% abundant (Fig. 1b), we cannot rule out the  
294 possibility that the stochasticity of sampling in OIL-PCR and the low abundance of this particular strain  
295 of *R. timonensis* precluded our ability to observe this association at the beginning of the time course.

## 296 Discussion

297 Here we show the ease with which OIL-PCR can identify novel carriers of known resistance markers on  
298 extrachromosomal elements within complex bacterial communities. We applied it to a neutropenic  
299 patient's microbiome and showed the correct association of three beta-lactamases with *K. pneumoniae*,  
300 and also discovered novel associations between these beta-lactamases and two gut commensals, *R.*  
301 *timonensis* and *Agathobacter* spp. Two of the genes, *bla*<sub>CTX-M</sub> and *bla*<sub>TEM</sub>, were both found on a large  
302 *Klebsiella* plasmid within the metagenome, suggesting the possible transfer of these genes to *R.*  
303 *timonensis* during the time course. Analysis of the plasmid sequence showed that it contains an origin of  
304 transfer, but does not have the genes necessary to transfer itself, meaning it would require a second  
305 "helper plasmid" to mobilize. Additionally, *bla*<sub>SHV</sub> was only found on a contig belonging to the *Klebsiella*  
306 genome without any known mobilizable transposons or integrative conjugative elements nearby, severely  
307 limiting its transfer potential. An alternative explanation for our results is that *Romboutsia* and *Klebsiella*  
308 became physically associated within the gut, and thus consistently emulsified together. Both of these  
309 explanations highlight the dynamic nature of the gut microbiome, either through horizontal gene transfer,  
310 or novel physical associations between pathogens and commensals, with close physical association being  
311 a known activator for conjugal transfer of genes<sup>26</sup>. In future applications of OIL-PCR, primers targeting  
312 non-transferrable genes could be used to distinguish between transfer and aggregation when identical  
313 genes are associated with different taxa.

314 Our results illustrate the application of a streamlined, simplified fusion PCR approach to obtain robust  
315 and sensitive associations of extrachromosomal DNA with bacterial hosts. It is a practical and  
316 transportable protocol with no requirements for specialized equipment nor specialized expertise. We  
317 identify improvements in performing single cell analysis on stool, namely the incorporation of a  
318 Nycodenz purification step and the incorporation of lysozyme plus heat-induced lysis. Additionally, we  
319 increased throughput at least three-fold through primer multiplexing and developed an automated protocol

320 to process at least 48 samples concurrently, allowing a total of 144 gene-sample association tests per  
321 batch.

322 Additional improvements to OIL-PCR could be explored to further increase throughput and sensitivity.

323 Although we tested multiplexing three genes per reaction, this number could likely be increased as we  
324 have found no sign of false positives due to multiplexing as demonstrated by associating a novel *bla*<sub>TEM</sub>  
325 variant with only *Escherichia* in time point T2 of patient B335 (Fig 2b, c). Further, we show that the OIL-  
326 PCR master mix facilitates permissive annealing of primers, allowing a mismatch one base from the  
327 primer's 3' end as demonstrated when *bla*<sub>OXY</sub> was detected in sample B324-2 with *bla*<sub>CTX-M</sub> primers.

328 These results could allow for the development of highly degenerate primers to target a broad range of  
329 gene variants. Non-specific priming during OIL-PCR is not of concern because the nested PCR reaction  
330 specifically filters out undesired fusion products. Lastly, the method described currently allows 40,000  
331 cells total per reaction. However, our TaqMan based qPCR assays suggest that the input concentration  
332 could be increased 10-fold by pre-treating cells with dsDNase (Supplementary Fig 4d). Combined with  
333 our result showing that OIL-PCR is more accurate when detecting low abundant taxa (Fig 1b), we feel  
334 confident that cell input can be increased to improve sensitivity without sacrificing accuracy.

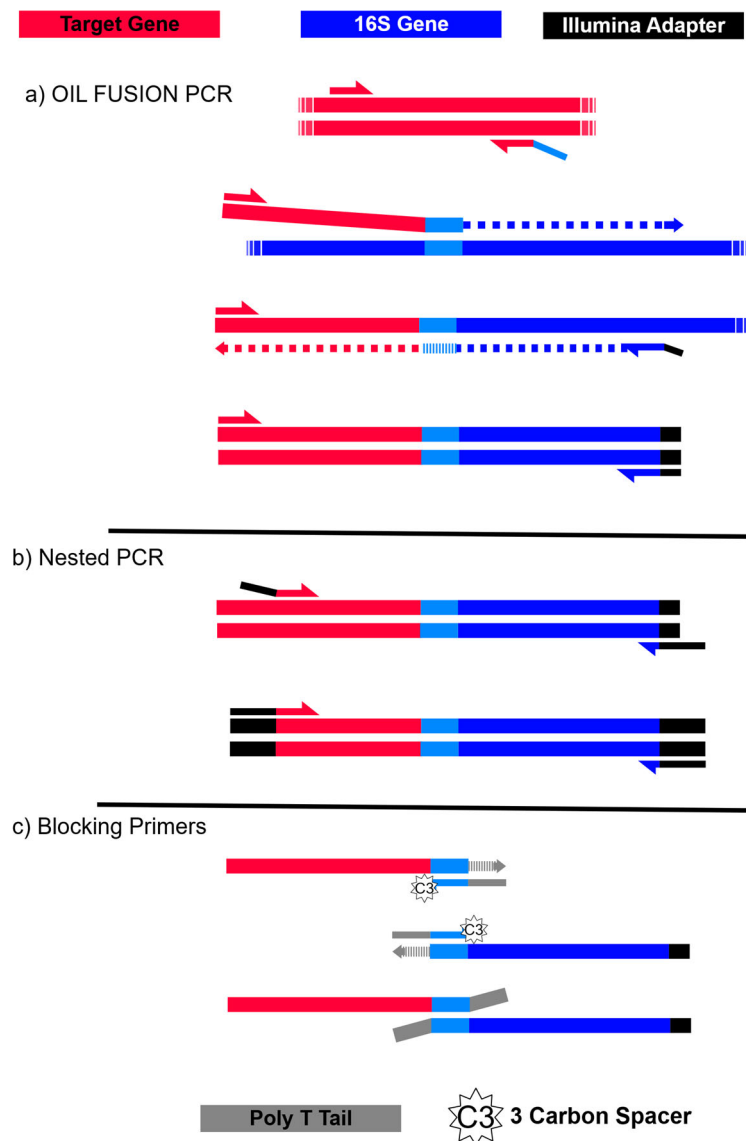
335 OIL-PCR is a highly versatile platform that could be applied across fields to address a multitude of  
336 questions. While we were interested in plasmid-born ARGs in the gut, the method could be used to target  
337 any gene of interest that is difficult to associate with a host using metagenomics. As mobile genetic  
338 elements are notoriously difficult to assemble due to their promiscuity which complicates de Bruijn graph  
339 assembly<sup>27</sup>, this method could be applied to find the hosts of integrated and non-integrated mobile  
340 elements. Similarly, as metavirome sequencing has revealed a massive number of viral genomes with  
341 unknown hosts<sup>28</sup>, OIL-PCR may be particularly useful in addressing this gap. Additionally, viral and  
342 plasmid host-range is an important determinant for understanding and modeling bacterial ecology of  
343 predation and HGT<sup>29</sup>. Further, targeting functional metabolic genes detected in metagenomes, but present  
344 at low abundance in bacterial communities, could identify novel bacteria involved in nutrient cycling



345 which has remained a persistent challenge in the field of bacterial ecology<sup>30</sup>. Finally, when combined with  
346 microfluidics, direct lysis of bacteria in an emulsion, as shown here, could be used to develop or simplify  
347 single-cell genome sequencing or single-cell RNA-seq for bacteria.

348

349 **Supplemental Figures**



350

351 **Supplemental Figure 1. Depiction of the fusion PCR reaction**

- 352 a) PCR is initialized with primers to a target gene (red). The reverse primer contains a 5' overhang  
353 complimentary to the universal V4 16S primer 519F (light blue). The product of this first  
354 amplification step can act as a forward primer for the 16S rRNA gene (blue). After extension of  
355 the full fusion product, the forward target primer can pair with the universal 16S reverse primer  
356 786R (with a portion of an Illumina TruSeq adapter sequence) to amplify the fully fused PCR  
357 product.
- 358 b) Nested PCR is performed on the fused PCR products from (a) in order to filter out non-specific  
359 priming from the fusion PCR. The forward primer anneals within the target gene and has a  
360 TruSeq adapter at the 5' end. The reverse primer also has the Illumina adapter sequence at its 5';  
361 end and anneals to the non-degenerate portion of 786R and the partial Illumina adapter sequence  
362 appended in (a).
- 363 c) Two blocking primers, both complementary to the 519F priming region, are included in the  
364 nested PCR to prevent unfused PCR products from annealing during the nested reaction.  
365 Blocking primers have a 3-carbon spacer on the 3' end to prevent extension and a poly-T tail that  
366 appends 10 As to the 3' end of any unfused products, thus inactivating them from annealing or  
367 extension.

368

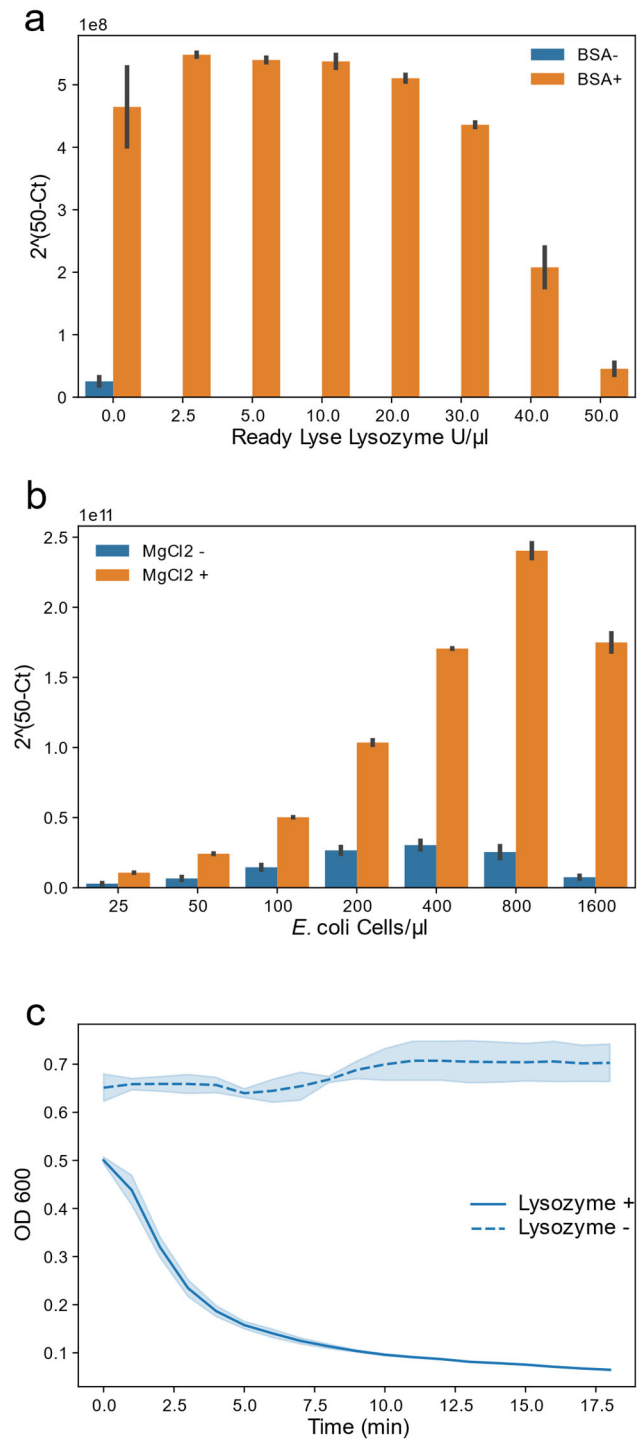
369

370

371

372

373



374 Supplemental Figure 2. BSA and excess MgCl<sub>2</sub> improve the efficiency of OIL-PCR and Ready Lyse

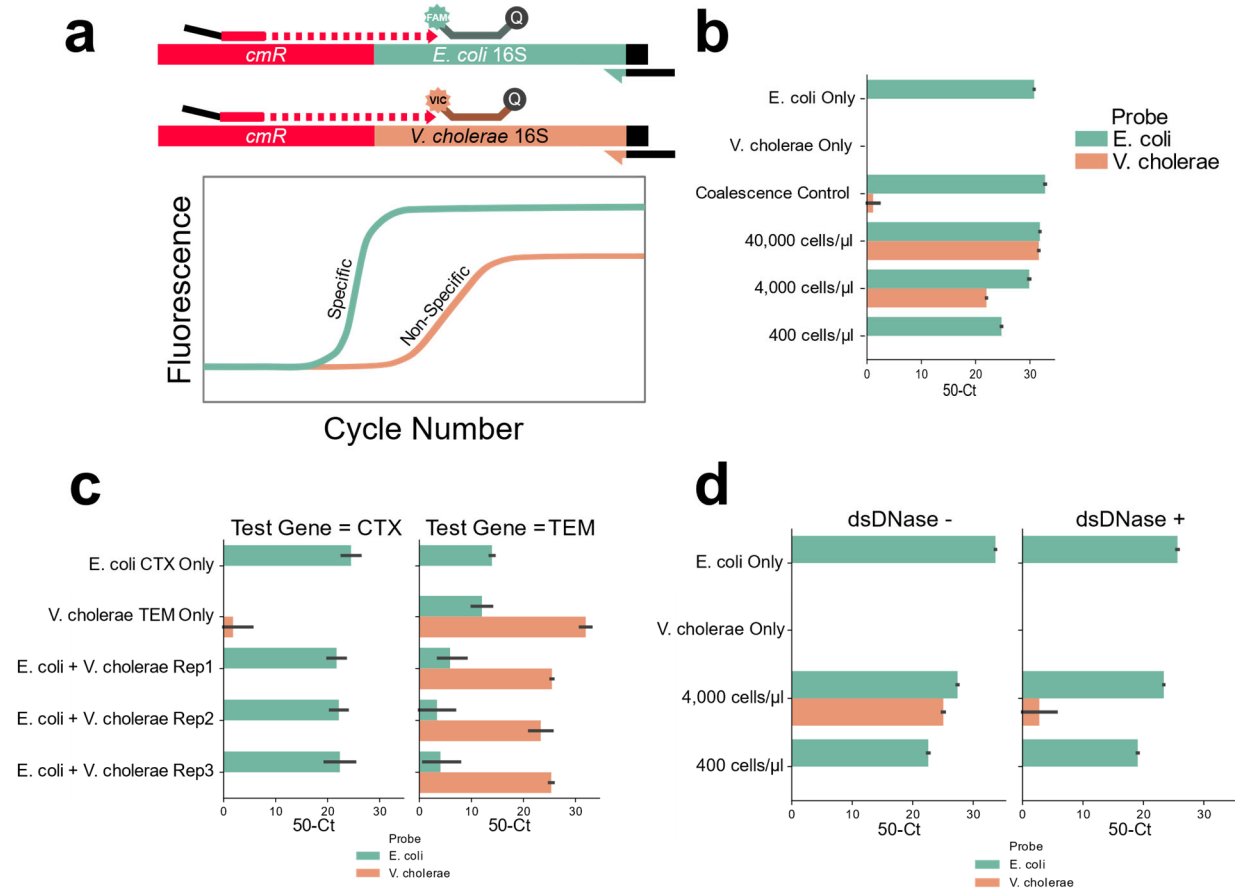
375 Lysozyme remains active in OIL-PCR master mix

- 376 a) Sybr-based qPCR was performed on the *cmR* gene carried on pBAD33 with varying  
377 concentrations of lysozyme in the presence (orange) or absence (blue) of BSA. Higher  $2^{(50-Ct)}$   
378 values represent greater amplification.
- 379 b) Sybr-based qPCR was performed on the *cmR* gene carried on the pBAD33 plasmid in *E. coli*  
380 MG1655 cells at increasing cell concentrations with (orange) and without (blue) additional  
381  $MgCl_2$ . Higher  $2^{(50-Ct)}$  values represent greater amplification.
- 382 c) Lysozyme activity against *B. subtilis* suspended in the OIL-PCR optimized reaction mix with  
383 (solid line) and without (dashed line) lysozyme.

384

385

386



387 **Supplemental Figure 3. Cell concentration of 400cells/μl, DNase treatment, and multiplexing PCR**  
 388 **reactions result in accurate OIL-PCR results**

- 389 a) Diagram of the Taqman assay used to monitor OIL-PCR results. Briefly, Taqman probes were  
 390 designed to be complementary for the 16S rRNA genes in either *E. coli* or *V. cholerae*, each with  
 391 its own fluorophore. OIL-PCR was performed on *E. coli* carrying the *cmR* gene on the pBAD33  
 392 plasmid but not present in *V. cholerae*. Fusion PCR products were recovered and nested probe-  
 393 based qPCR was performed. Upon amplification of the gene, the probe is cleaved by Taq  
 394 polymerase releasing the fluorophore from the quencher. Specific amplification of the designated  
 395 region is measured by fluorescence of the expected fusion product vs the non-specific product.
- 396 b) OIL-PCR with primers targeting a plasmid-borne *cmR* gene was performed with a 1:1 mix of  
 397 *cmR* positive *E. coli* and *cmR* negative *V. cholerae* cell suspensions with. A gradient of cell

398 concentrations was tested (400-40,000 cells/ $\mu$ l), in addition to *E. coli* and *V. cholerae* suspensions  
399 alone as positive and negative controls. Control emulsions were mixed 1:1 after emulsification to  
400 test for droplet coalescence.

401 c) Multiplexed OIL-PCR was performed with primer sets targeting a genomic *bla<sub>CTX-M</sub>* gene in *E.*  
402 *coli* and a plasmid-borne *bla<sub>TEM</sub>* gene in *V. cholerae*. Experiments were performed in triplicate  
403 and on each of the organisms separately. Results are shown for the *bla<sub>CTX-M</sub>* (left) and *bla<sub>TEM</sub>*  
404 (right).

405 d) OIL-PCR with primers targeting a plasmid-borne *cmR* was performed after pretreating cells with  
406 (right) and without (left) dsDNase at two different 1:1 *E. coli* to *V. cholerae* cell suspension  
407 concentrations as well as on the individual bacterial strains for controls.

408

409

410

411

412

413

414

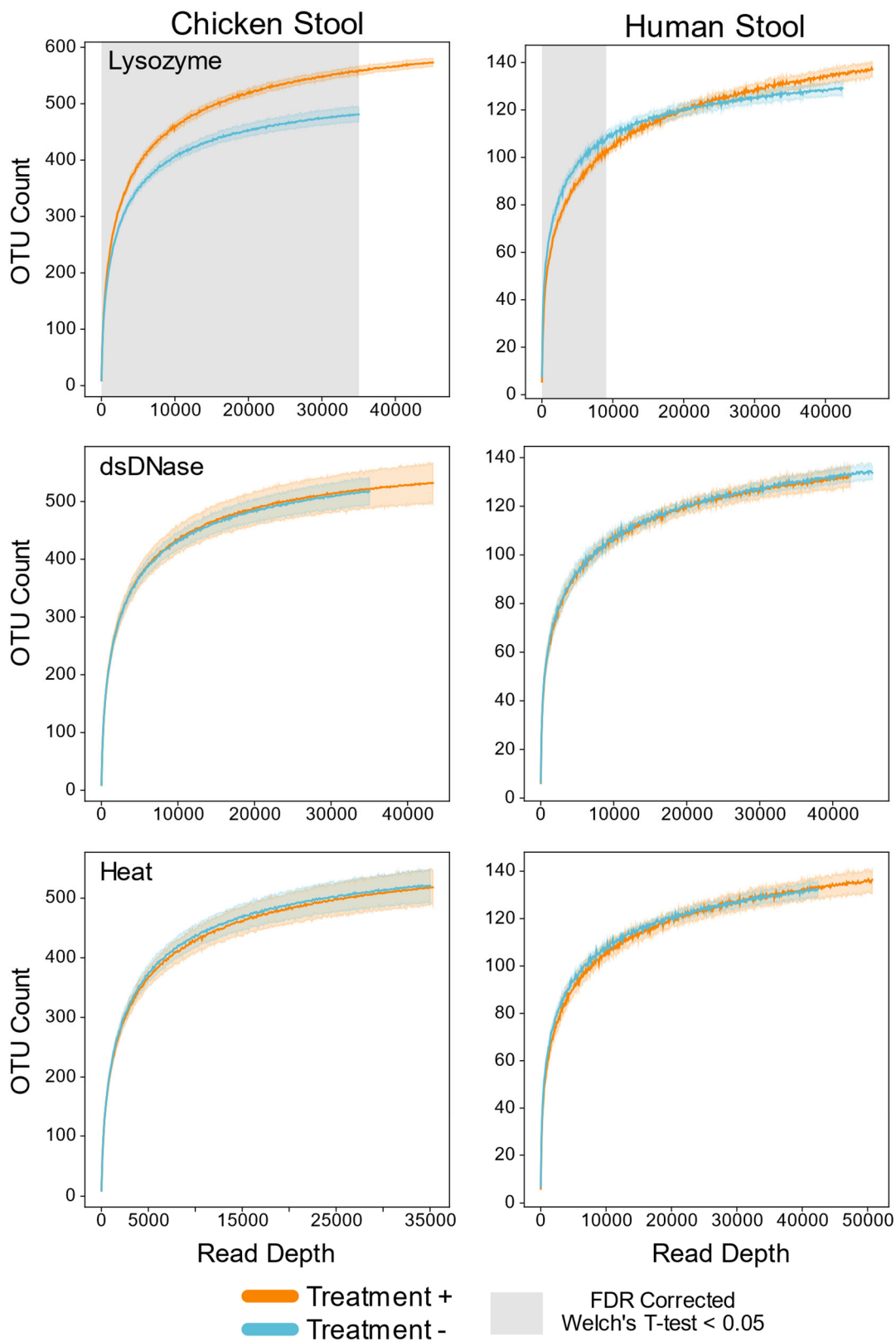
415

416

417

418

419

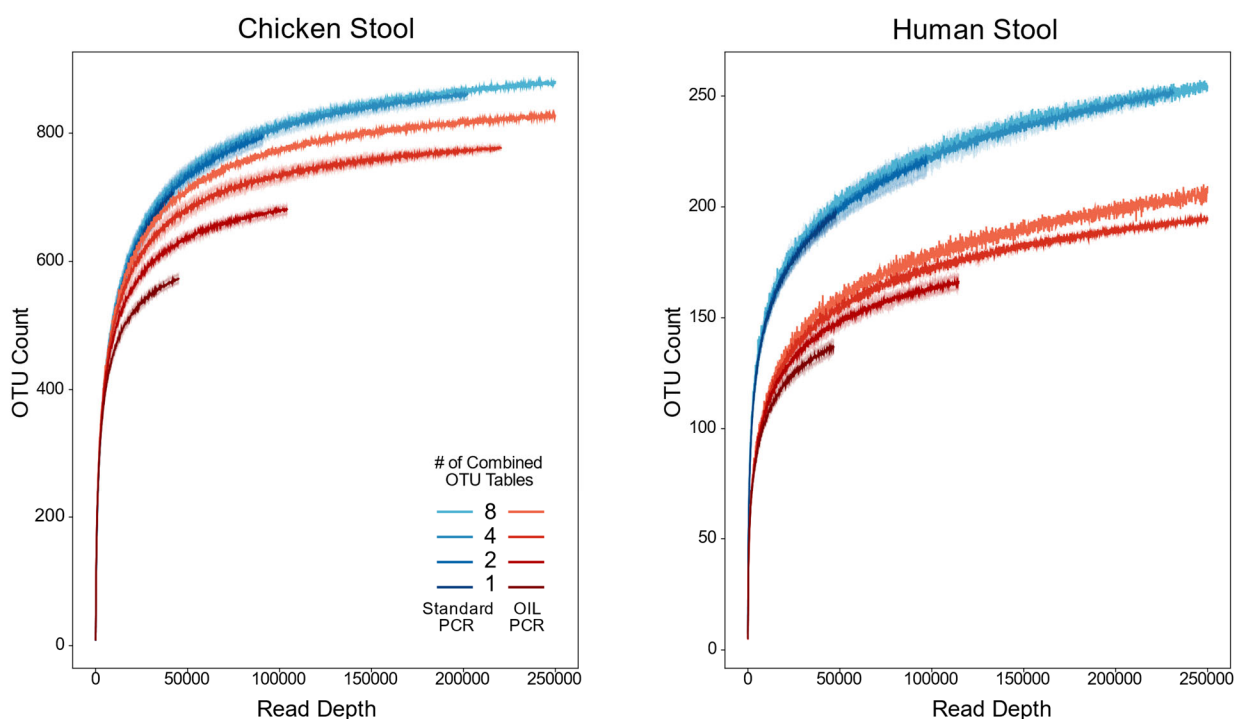


421 **Supplemental Figure 4. Lysozyme alone improved recovery of species.**

422 Rarefaction analysis of chicken (left) or human (right) gut microbiome samples with (orange) and without  
423 (blue) lysozyme (top), dsDNA treatment (middle) and heat (bottom). Grayed regions in the plot represent  
424 areas where the curves are significantly different from one another ( $p < 0.05$ ), according to an FDR-  
425 corrected Welch's t-test.

426

427



428

429 **Supplemental Figure 5. Combining replicates for increased depth improved recovery of species and**  
430 **reduced stochastic sampling bias.**

431 Rarefaction analysis of chicken (left) or human (right) gut microbiome samples performed with OIL-PCR  
432 (red) or standard DNA extraction and library prep (blue). OTU tables were repeatedly subsampled in  
433 groups of 2, 4, or 8 replicates from 8 total replicate 16S libraries.



434 **Methods**

435 **Optimizing OIL-PCR Reaction Buffer for Phusion and RL Lysozyme Compatibility**

436 SYBR-Based qPCR Assay for Phusion Polymerase Activity with Lysozyme

437 SYBR-based qPCR reactions were set up in duplicate as follows: 25 µl reactions with 20 U/ml Phusion  
438 Hot Start Flex DNA polymerase (NEB M0535L), 1X HF Buffer, 200 µM dNTP mix (NEB N0447L), 400  
439 nM of 519F and 786R, 1X SYBR Green (Thermo Fisher S7563), 1X ROX reference dye (Thermo Fisher  
440 12223012), 0.5 mg/ml of BSA (NEB B9000S) when included, 0.01% Triton-X 100, and 1µl of template  
441 DNA. Reactions were prepared with 0, 2.5, 5, 10, 20, 30, 40 and 50 U/µl of Ready-Lyse Lysozyme  
442 (Lucigen R1810M). qPCR was performed on the Thermo Fisher Quant Studio 3 Real-Time PCR machine  
443 with the following parameters: 98 °C for 1 minutes, then 50 cycles of 98 °C for 5 seconds, 54 °C for 30  
444 seconds, and 72 °C for 30 seconds. Proper amplification was confirmed using melt curves: 98 °C for 5  
445 seconds, cool to 60 °C at 1.6 °C/s, and then heat to 95 °C at 0.15 °C /s. Ct values and melt curves were  
446 generated with the Quant Studio software V1.4 using the default software settings.

447 Lysozyme Activity Assay in OIL-PCR Master Mix

448 Lysozyme testing was performed in a lysozyme test buffer made from the OIL-PCR master mix with  
449 dNTPs, primers, and Phusion polymerase replaced with water and 100% glycerol (48ul/ml). Log phase  
450 cultures of *B. subtilis* were standardized to an OD<sub>600</sub> of 2 and suspended in 1x Lysozyme test buffer.  
451 Separately, lysozyme was suspended in 1x Lysozyme test buffer at 2x concentration. 100µl of the  
452 lysozyme mix was aliquoted into a 96-well, clear, flat-bottomed microtiter plate before adding 100µl of  
453 suspended culture. Lysis was monitored using a Spectramax M3 plate reader (Molecular Devices), heated  
454 to 37 °C and OD<sub>600</sub> measured every minute for an hour.

455

456

#### 457 Optimizing OIL-PCR Reaction Efficiency in an Emulsion

458 50µl PCR reactions were prepared in 1.5 ml tubes as describe in the Tube-Based OIL-PCR method below  
459 with varying concentrations of Phusion polymerase, bovine serum albumin (BSA), Ready Lyse lysozyme,  
460 dithiothreitol (DTT), MgCl<sub>2</sub>, dNTPs, and ammonium sulfate. *E. coli* genomic DNA was used as template  
461 and amplified with universal 16S primers 519F and 796R. Reactions were emulsified 25 Hz for 30  
462 seconds before aliquoting to PCR tubes and thermocycling. Final PCR products were separated from the  
463 emulsion as describe below and amplification efficiency was assessed quantitatively by SYBR-based  
464 qPCR or qualitatively by gel image band intensity.

#### 465 Emulsion Stabilization Experiments

466 OIL-PCR test buffer was prepared similarly to the lysis activity assays with ether NEB HF buffer, or  
467 Detergent Free Buffer (Thermo Fisher F520L), while omitting bacterial cells or RL Lysozyme. Reactions  
468 were emulsified at 25 Hz for 30 seconds on a Retch Mixer Mill MM 400 with adapters 11990 and 11993  
469 (Mobio/Qiagen). Emulsion tubes were photographed before and after thermocycling and assayed by eye  
470 for coalescence. After confirming a stable emulsion, qPCR and lysis time series experiments were  
471 repeated to confirm activity of Phusion DNA polymerase and RL Lysozyme in the DF buffer.

#### 472 **OIL-PCR in Tube Based Format for Master Mix Optimization**

##### 473 Fusion PCR Reaction Setup

474 All steps were performed on ice or in a 4°C centrifuge until after emulsification. 50 µl PCR reactions  
475 were prepared in a 1.5 ml microcentrifuge tube with varying experimental conditions. 2 µl of bacterial  
476 cells standardized to 10<sup>4</sup> cells/µl were added to 48 µl of master mix and vortexed to evenly disperse cells  
477 before adding 300 µl of cold Droplet Generation Oil for Probes (BioRad 1863005). Emulsions were  
478 formed immediately after by shaking tubes at 25 Hz for 30 seconds on a Retch Mixer Mill MM 400 with  
479 adapters 11990 and 11993 (Mobio/Qiagen). Next, the emulsion mix was divided into four 70 µl aliquots  
480 in a PCR strip-tube and thermocycled as follows: 37 °C for 5 minutes, 95 °C for 10 minutes, then 38

481 cycles of 95 °C for 5 seconds, 54 °C for 30 seconds, and 72 °C for 30 seconds, followed by final  
482 extension 72 °C for 2 minutes. After PCR amplification, the aliquots were briefly vortexed and pooled  
483 into a clean 1.5 ml microcentrifuge tube. To break the emulsion, 50 µl of TE and 70 µl of  
484 Perfluorooctanol (Krackeler Scientific 45-370533-25G) were added and the mixture was vortexed  
485 vigorously for 30 seconds. Tubes were centrifuged at 5000 G for 1 minute and the upper aqueous phase  
486 was transferred to a new PCR strip tube and purified using AMPure XP beads as described below.

#### 487 Manual AMPure XP Bead cleanup

488 AMPure XP beads (Beckman A63880) were added at a ratio of 0.8 µl beads per 1 µl of recovered DNA,  
489 vortexed, and incubated for 5 minutes for DNA binding. PCR strip tubes were transferred to a 96-Well  
490 magnet (Eppendorf Magnum FLX) to pull down beads for 5 minutes. Supernatant was removed with a  
491 multichannel pipette and the pellet was washed twice with 100 µl of 70% EtOH before drying for 10  
492 minutes at room temperature. The bead pellet was suspended in 20 – 50 µl of TE and incubated for 5  
493 minutes to elute DNA, before returning to the magnet and transferring supernatant to fresh PCR strip  
494 tubes. Eluted DNA was either run directly on a gel for qualitative analysis of amplification, or used as  
495 template in qPCR assays.

#### 496 **Probe-Based qPCR with TaqMan Probes for Cell Input Optimization and Multiplexing**

##### 497 Standardization of Bacterial Test Strains

498 For all experiments, bacterial type strains *Escherichia coli* MG1655<sup>19</sup>, *Vibrio cholerae* N16961<sup>31</sup>, and  
499 *Bacillus subtilis* 168<sup>32</sup> were inoculated from frozen glycerol stocks into 5 ml LB and grown at 37 °C  
500 overnight. Cultures were diluted 1:100 in 5ml fresh LB the next day and grown to OD<sub>600</sub> 0.4-0.8. CFU/µl  
501 at OD<sub>600</sub> was quantified by serial dilution of cells in LB, plating, and colony counting. Count results were  
502 used to standardize cell cultures to a stock concentration of 10<sup>6</sup> CFU/µl to be diluted and used as input for  
503 OIL-PCR.

504

505 Optimizing Cell Input Concentration

506 Cultures of WT *V. cholerae* N16961<sup>31</sup> and *E. coli* MG1655<sup>19</sup> carrying plasmid pBAD33<sup>20</sup> with *cmR* were  
507 standardized to 10<sup>4</sup>, 10<sup>5</sup>, and 10<sup>6</sup> CFU/μl in LB. The two strains were mixed 1:1 at each of the three  
508 concentrations, and 2 μl of cells was used as template in 50 μl tube-based OIL-PCR reactions with fusion  
509 primers targeting the *cmR* gene. Reactions with each strain emulsified individually were run as controls.  
510 Droplet coalescence was assayed by mixing individual control reactions after emulsification, thereby  
511 ensuring the two strains were not encapsulated together. Reactions were thermocycled and recovered  
512 DNA was used as template in the probe-based qPCR to quantify specific vs non-specific fusion products.

513 Probe-Based qPCR Assay

514 Probes were designed to target unique regions of *E. coli* and *V. cholerae* 16S ribosomal rRNA gene. Both  
515 probes hybridized to the antisense strand and can only be cleaved when the polymerase extended from the  
516 nested *cmR* primer, across the fusion junction, and into the 16S gene, thus distinguishing actual fused  
517 PCR products from stray fragments of 16S DNA. Probes were verified to only target their specified  
518 strain, with the *V. cholerae* probe having a VIC/NFQ MGB reporter probe and *E. coli* a FAM/NFG MGB  
519 probe. 20 μl qPCR reactions were prepared in duplicate as follows: 1x Luna Universal Probe qPCR  
520 Master Mix (NEB M3004L), 300 nM of forward and reverse primer, 3.2 μM of forward and reverse  
521 blocking primers, 200 nM of *E. coli* and *V. cholerae* TaqMan probes, and 2-5 μl of recovered OIL-PCR  
522 amplicons. Reactions were amplified under the following conditions: 95 °C for 1 minutes, then 50 cycles  
523 of 95 °C for 20 seconds, 55 °C for 20 seconds, and 60 °C for 20 seconds. For analysis, Ct values were  
524 subtracted from the total number of cycles for easier interpretation.

525 Primer Multiplexing Validation

526 Four strains of bacteria were used to test primer multiplexing: *V. cholerae* N16961<sup>31</sup> carrying *ampR* on  
527 RP4 plasmid<sup>33</sup>, WT *V. cholerae* N16961, *E. coli* 0006 (CDC & FDA Antibiotic Resistance Isolate Bank)  
528 carrying *bla*<sub>CTX-M-15</sub>, and WT *E. coli* MG1655<sup>19</sup>, all mixed at a ratio of 1:49:10:40 with a final

529 concentration of  $10^4$  cells/ $\mu$ l. This mix of cells resulted in 10% of the consortium carrying *bla*<sub>CTX-M-15</sub> and  
530 1% carrying *amrR* to provide a more realistic depiction of the abundances of ARGs in natural stool  
531 communities. OIL-PCR was performed in a plate-based format with forward and fusion primers for both  
532 *amrR* and *bla*<sub>CTX-M-15</sub>. Each strain was tested individually as controls. Purified fusion products were  
533 assayed for correct fusions using the probe-based qPCR assay with nested primers targeting *amrR* or  
534 *bla*<sub>CTX-M-15</sub> in parallel reactions.

### 535 **Final OIL-PCR Parameters:**

#### 536 OIL-PCR:

537 The final, optimized OIL-PCR master mix is as follows: 100 U/ $\mu$ l Phusion Hot Start Flex DNA  
538 Polymerase, 1X DF Buffer (Thermo Fisher F520L), 250  $\mu$ M dNTPs (NEB N0447L), 2  $\mu$ M universal 16S  
539 reverse primer 786R, 1  $\mu$ M of each target specific forward primer, 0.01  $\mu$ M of each target specific fusion  
540 primer with universal 519F' tail, 1.5 mM additional MgCl<sub>2</sub>, 5mM Ammonium Sulfate, 5 mM DTT, 4  
541 mg/ml BSA (NEB B9000S), 300 U/ $\mu$ l RL Lysozyme, 400 cells/ $\mu$ l Nycodenz purified cells. 300  $\mu$ l  
542 emulsion oil (BioRad 1863005) was added to 50  $\mu$ l reactions when performed in individual tubes, or 200  
543  $\mu$ l of emulsion oil was added to 100  $\mu$ l OIL-PCR reactions when performed in the 96-well plate format.  
544 Tubes were emulsified at 25 Hz for 30 seconds, while plates were sealed with a 50  $\mu$ m aluminum seal  
545 (Axygen PCR-AS-600) and emulsified for 2 rounds of 27.5 Hz for 20 seconds; flipping the plate in  
546 between for consistent emulsion across rows.

547 The lysis and amplification program is: 37 °C for 5 minutes, 95 °C for 10 minutes, then 38 cycles of 95  
548 °C for 5 seconds, 54 °C for 30 seconds, 72 °C for 30 seconds, before final extension of 72 °C for 2  
549 minutes.

#### 550 dsDNase Treatment and Heat Inactivation in OIL-PCR

551 dsDNase treatment was not used in the initial OIL-PCR optimization or spike-in experiments. Cells were  
552 standardized to  $10^4$  cells/ $\mu$ l in 100  $\mu$ l of PBS. 1  $\mu$ l of stock dsDNase (Thermo Fisher EN0771) was added

553 to the tube and incubated at room temp for 10 minutes before returning to ice. Treated cells were used  
554 directly in OIL-PCR. The enzyme was inactivated immediately after emulsification (optional) by  
555 incubating 10 minutes in a water bath set exactly to 50 °C with gentle mixing by hand every 2 minutes.

556 Nested PCR:

557 SYBR-based qPCR was performed on purified fusion PCR products to minimize the number of cycles for  
558 each reaction with the goal of reducing chimera formation. Amplification was performed in 20 µl  
559 reactions using the Luna Universal qPCR Master Mix (NEB M3003L) with 1x PCR master mix, 300 nM  
560 forward and reverse primers, and 2-5 µl of purified template. For multiplexed experiments, separate  
561 reactions were prepared, with one set of nested primers for each gene assayed. The following  
562 thermocycling conditions were used: 95 °C for 2 minutes, 40 cycles of 95 °C for 15 seconds, 55 °C for 15  
563 seconds, 68 °C for 20 seconds, followed by a final extension phase at 68 °C for 1 minutes. Melt curves  
564 were measured by heating to 95 °C at 0.15 °C /s. Blocking primers were not included in SYBR-based  
565 qPCR reactions because of the strong signal from self-hybridization. Ct values were used to select the  
566 cycle number for nested amplification that was equal to the Ct value +/- 2 cycles. Reactions that did not  
567 amplify in the qPCR were amplified with the highest number of cycles for that preparation.

568 Using the qPCR results to select the cycle number, nested PCR reactions were prepared in duplicate 20 µl  
569 reactions as follows: 20 U/ml Phusion DNA polymerase, 1x HF Buffer, 2 µM dNTPs, 300 nM target gene  
570 specific forward primer and universal reverse primer, 32 µM of each blocking primer, and 2-5 µl of  
571 template. Thermocycling was performed with variable number of cycles based on the qPCR as follows:  
572 98 °C for 3 minutes, then variable cycles of 98 °C for 5 seconds, 55 °C for 30 seconds, and 72 °C for 30  
573 seconds, followed by final extension 72 °C for 5 minutes. Duplicate PCR reactions were pooled and  
574 purified using automated AMPure XP cleanup.

575

576

## 577 Illumina Indexing PCR and Library Preparation

578 Custom indexing primers were designed based on Spencer et al<sup>11</sup>. A set of unique, 9 bp barcodes was  
579 generated using Barcode Generator V2.8<sup>34</sup>. The primers are compatible with the Illumina Truseq primers  
580 and the index can be read with 8 bp instead of 9 to make them compatible with other libraries.

581 Indexing PCR was performed with 25 µl reactions as follows: 20 U/ml Phusion DNA polymerase, 1x HF  
582 Buffer, 2 µM dNTPs, 100 nM of unique forward and reverse indexing primers, and 2 µl of purified nested  
583 PCR template. Cycling was performed as follows: 98 °C for 1 minutes, then 20 cycles of 98 °C for 15  
584 seconds, 56 °C for 30 seconds, and 72 °C for 45 seconds, followed by final extension 72 °C for 2 minutes.  
585 PCR reactions were purified using automated AMPure XP cleanup.

586 Indexed PCR libraries were quantified using QUANT-IT pico green dsDNA assay kit (Invitrogen P7589)  
587 and measured on the Spectramax M3 plate reader. Wells were pooled based on the measured  
588 concentration using the Eppendorf epMotion 5075vte robot and the final pool quantified using the Qubit  
589 Broad Range Assay Kit (Thermo Fisher Q32853). Pools were run on a gel to confirm clean DNA before  
590 sequencing with MiSeq 2x250 V2 chemistry.

## 591 **Plate-Based OIL-PCR With Robotic Automation:**

### 592 Reaction Setup

593 96 µl of the final OIL-PCR master mix was aliquoted into a 500 µl deep well plate (Eppendorf 00.0  
594 501.101). Nycodenz purified stool cells were diluted in PBS to 10<sup>4</sup> cells/µl in an 8-well PCR strip for  
595 multichannel pipetting. 4 µl of cells was quickly added to the reactions with a 10 µl 8-channel pipette  
596 before sealing with an extra-thick foil seal (Axygen PCR-AS-600) and vortexed to mix. The reactions  
597 were briefly centrifuged to return liquid to the bottom of the plate, and then placed on an orbital  
598 microplate shaker (VWR 12620-926) at 1200 rpm for 30 seconds to further mix the cells while keeping  
599 the mix at the bottom of the wells. After mixing, the foil seal was carefully removed and 200 µl of cold  
600 emulsion oil was added using a multichannel pipette. The plate was then sealed with a fresh foil seal and

601 shaken at 27.5 Hz for 20 seconds on the Retch shaker MM 400 with plate adapter (#11990). The plate  
602 was removed and turned over to shake an additional 20 seconds providing an even emulsion across the  
603 plate. After emulsifying, each reaction was aliquoted into 4 wells of a PCR plate (Eppendorf 0030  
604 128.648) using the robot for consistency. The plates were sealed and run on the OIL-PCR fusion program  
605 described earlier.

#### 606 DNA Recovery from Emulsion

607 After amplification, the robot was used to purify the OIL-PCR Products. In short, replicate reactions were  
608 pooled into a fresh 500 µl deep well plate, and 60 µl of TE and 70 µl of Perfluorooctanol (Krackeler  
609 Scientific 45-370533-25G) were added to each well. The plate was sealed and shaken on the Retch at 30  
610 Hz for 40 seconds to thoroughly disrupt the emulsion. The plate was then centrifuged in a swing bucket  
611 rotor at 5000 Gs for 1 minute to separate the phases and returned to the robot. 80 µl of the upper phase  
612 was aspirated from a defined height into a fresh 500 µl deep well plate for automated Ampure XP bead  
613 purification.

#### 614 Automated AMPure XP Bead Purification

615 85 µl of AMPure XP beads (Beckman A63880) was added to the deep well plate containing the recovered  
616 OIL-PCR fusion products. The reactions were mixed at 1200 rpm for 1 minute and incubated for 2  
617 minutes for DNA binding, before transferring to the magnet (Eppendorf Magnum FLX) for 3 minutes.  
618 After pulldown, the supernatant was discarded and the wells were washed twice with 200 µl of 70%  
619 EtOH. After discarding the second wash, the plate was removed from the magnet and dried at room temp  
620 for 10 minutes before adding 50 µl of TE buffer. The plate was shaken at 1200 rpm for 1 minute and  
621 incubated 2 minutes to elute the DNA. Finally, the plate was returned to the magnet and for 2 minutes and  
622 48 µl of purified DNA was transferred to a fresh 96-well PCR plate (Eppendorf 0030 128.648).

623



## 624 **OIL-PCR on Natural Stool Communities**

### 625 Nycodenz Purification of Stool Cells

626 All steps were performed on ice and in a 4c refrigerated centrifuge unless otherwise noted. Stool samples  
627 were collected in PBS + 20% glycerol + 0.1% L-cysteine and frozen at -80c until processed. Frozen  
628 samples were thawed completely and thoroughly homogenized via vortexing. Samples were diluted at  
629 least 1:1 in cold PBS to reduce the sample viscosity and glycerol concentration as viscous samples did not  
630 to separate well with the Nycodenz. Samples were vortexed at maximum speed for 5 minutes to release  
631 cells from stool particles. 300µl of cold 80% Nycodenz (VWR 100356-726) was aliquoted to the bottom  
632 of 2 ml microcentrifuge tubes and 1.6 ml of stool slurry was overlaid on top without mixing the two  
633 phases. Tubes were centrifuged at 10,000 G for 40 minutes in a swing bucket rotor to separate cells. After  
634 centrifugation, the upper phase was removed with a pipette and 500µl of cold PBS was used to wash the  
635 bacterial cell pellet from the insoluble stool fraction. The suspended cells were removed and the pellet  
636 was washed a second time with 500 µl of PBS. Cells were centrifuged at 50g for 1 minute to pellet any  
637 large particles that carried over from the Nycodenz purification and the upper phase was passed through a  
638 40 µm nylon mesh screen (Falcon 352235) to remove any residual stool debris or large cell clumps.  
639 Samples of each preparation were diluted 1:1 PBS + 20% glycerol for whole cell storage. Lastly, purified  
640 cells were diluted and imaged at 100x magnification within a 20 µm counting chamber (VWR 15170-  
641 048). Images were analyzed using FIJI/ImageJ 1.52p (Java 1.8.0\_172) to manually count cells and  
642 calculate cell concentration in glycerol stocks.

### 643 Spike-In Experiment

644 This experiment was performed using the individual tube-based format of OIL-PCR. Nycodenz purified  
645 stool and *E. coli* carrying pBAD33<sup>20</sup> with *cmR* was standardized to 10<sup>4</sup> cells/µl. *E. coli* cells were mixed  
646 with the stool samples at a ratio of 1:10, 1:100, and 1:1000, and the mixed cultures were added to OIL-  
647 PCR containing the *cmR* primer set. Reactions were emulsified, lysed, thermocycled, and fusion products

648 were purified manually. Nested PCR was performed with the nested *cmR* primer before indexing,  
649 pooling, and sequencing.

#### 650 Lysozyme, dsDNase, Heat Experiment

651 Nycodenz-purified human and chicken stool cells were standardized to  $10^5$  cells/ $\mu$ l and incubated with or  
652 without dsDNase at room temp for 10 minutes. OIL-PCR master mix was prepared with and without  
653 Lysozyme using universal 16S rRNA primers i519F and i786R. Cells were added to the OIL-PCR  
654 reaction and emulsified. Emulsions were either incubated at 50 °C or room temperature for 10 minutes  
655 before aliquoting to PCR plates and running the OIL-PCR fusion program. Amplicons were purified,  
656 indexed, and submitted for Illumina sequencing as described above.

#### 657 **OIL-PCR for Detection of *bla* genes in Neutropenic Patients**

##### 658 Sample collection and Metagenomic Assemblies

659 Samples were collected, sequenced, and metagenomic assemblies were prepared as described in Kent et  
660 al.<sup>2</sup> Briefly, serial stool samples were collected from consenting individuals receiving a hematopoietic  
661 stem cell transplant at NewYork-Presbyterian Hospital/Weill Cornell Medical Center in accordance with  
662 IRB protocols for Weill Cornell Medical College (#1504016114) and Cornell University (#1609006586).  
663 Samples were either frozen “as is” (for metagenomic sequencing) or homogenized in phosphate-buffered  
664 saline (PBS) + 20% glycerol before freezing (for OIL-PCR). DNA was isolated from samples destined for  
665 metagenomic sequencing using the PowerSoil DNA Isolation Kit (Qiagen) with additional proteinase K  
666 treatment and freeze/thaw cycles recommended by the manufacturer for difficult-to-lyse cells. Extractions  
667 were further purified using 1.8 volumes of Agencourt AMPure XP bead solution (Beckman Coulter).  
668 DNA was diluted to 0.2 ng/ $\mu$ L in nuclease-free water and processed for sequencing using the Nextera XT  
669 DNA Library Prep Kit (Illumina).

670

671 Design and Validation of OIL-PCR fusion primers

672 ARG variants for the three *bla* genes were downloaded from the CARD database<sup>35</sup> and aligned in  
673 Snapgene using default MUSCLE parameters. Conserved regions were identified manually and  
674 degenerate primers were designed to capture as many variants of the genes as possible. Primers were  
675 selected for GC content between 40 – 60% and an annealing temperature of 58 °C based on the Snapgene  
676 calculation. Degenerate bases were limited to 3 per primer and no less than 5 bp from the 5' end.

677 Strains acquired through the CDC & FDA Antibiotic Resistance Isolate Bank carrying multiple variants  
678 of each gene (Supplementary Table T1)) were used as template for testing *bla* primers. At least 3 sets of  
679 primers were designed and tested in every possible combination using the OIL-PCR master mix without  
680 emulsion to find a set of three primers that provided clean fusion amplification. Lastly, working primer  
681 sets were tested in an emulsion on whole cells to confirm amplification in OIL-PCR.

682 Fusion Primers targeting Tn3 transposon genes were designed using scaffolds from the metagenomic  
683 assemblies and tested on *Klebsiella* isolate DNA from patient B335.

684 OIL-PCR on Neutropenic Patients

685 All OIL-PCR reactions were performed with the plate-based protocol including dsDNase treatment and  
686 heat inactivation. Whole bacterial cells were purified with Nycodenz, quantified and standardized to 10<sup>4</sup>  
687 cells/μl in PBS before treating with dsDNase. For multiplexed experiments, reactions were prepared in  
688 quadruplicate with three sets of primers targeting the three *bla* genes in each reaction. The singleplex  
689 reactions were prepared in triplicate with only one primer set per reaction. In all cases, the reactions  
690 followed the standard plate-based protocol with automation, including heat inactivation of the dsDNase  
691 after emulsification. Nested PCR, indexing, and library preparation was performed as described above.

692

693

## 694 Romboutsia Specific OIL-PCR

695 CRIB primers<sup>25</sup> were modified to form a fusion product with all three *bla* genes, however, only the *bla*<sub>TEM</sub>  
696 primer set amplified when tested. Using only the *bla*<sub>TEM</sub> primer set, OIL-PCR was performed with  
697 dsDNase treatment, in triplicate, using the plate-based format with automation. Nested PCR, indexing,  
698 and library preparation was performed as described above.

## 699 **Computational Methods**

### 700 Processing 16S rRNA Sequencing

701 Raw reads were merged using usearch<sup>36</sup> (V 11.0.667) -fastq\_mergepairs (maxdiffs: 20, pctid: 85,  
702 minmergelen: 283, maxmergelen: 293) before trimming primers and quality filtering with usearch -  
703 fastq\_filter (maxee: 1.0). Unique reads were filtered using usearch -fastx\_uniques and OTUs were  
704 clustered based on 97% identity with usearch -cluster\_otus. OTU tables were generated with usearch -  
705 otutab and taxonomy was assigned with RDP classifier implemented in MOTHUR classify.sequs (1.38.1)  
706 against silva v132. Rarefaction curves were generated using QIIME1<sup>37</sup> (v1.9) multiple\_rarefaction.py (-m  
707 10, -x 100000, -s 100, -n 5, -k).

### 708 Processing OIL-PCR Sequencing

709 Raw reads were merged using usearch<sup>36</sup> (V 11.0.667) -fastq\_mergepairs (maxdiffs: 10% of expected  
710 overlap, pctid: 85, minmergelen: expected length-15, maxmergelen: expected length +15) before  
711 trimming primers and quality filtering with usearch -fastq\_filter (maxee: 1.0). Unique reads were filtered  
712 using usearch -fastx\_uniques. Reads were split at the fusion junction into 16S and target reads using  
713 cutadapt V2.1<sup>38</sup> because of its tolerance for PCR errors which are often introduced in the fusion junction  
714 of the OIL-PCR amplicons. The 16S reads were clustered based on 97% identity with usearch -  
715 cluster\_otus, OTU tables were generated with usearch -otutab and taxonomy was assigned with RDP  
716 classify implemented in mothur<sup>39</sup> classify.sequs (1.38.1) against SILVA<sup>40</sup> v132. Target reads were  
717 identified by blasting against a custom database of expected sequences with blastn<sup>41</sup> (v2.9.0). 16S

718 taxonomy and target read identity were then reassociated using a custom python script to parse the files.  
719 Detections were defined by taxa – target associations that make up 0.5% of the total reads across  
720 replicates.

#### 721 Strain Level Analysis of *Romboutsia* in Metagenomes

722 Metagenomic reads from each time point were aligned to the *R. timonensis* reference genome (Refseq  
723 accession code: GCF\_900106845.1) using BWA mem (v0.7.17, -a)<sup>42</sup>. Reads aligning to the reference  
724 genome were then assembled using SPAdes (v3.14.)<sup>43</sup>. To determine the presence and identity of strains  
725 from each time point, AMPHORA<sup>44</sup> (v2, marker identification step only) was used to identify the  
726 sequences of 30 marker genes within each assembled *R. timonensis* genome. The marker genes identified  
727 by AMPHORA were then mapped (Diamond, v2.0.4)<sup>45</sup> to the BLAST<sup>46</sup> nr database for taxonomic  
728 annotation (BLAST nr database downloaded 2018). DNA sequences of the marker genes that mapped to  
729 *R. timonensis* were retained for further analysis. Genes from time point 2 and time point 2 were aligned to  
730 one another (BLAST blastn, v2.9.0)<sup>41</sup>, and then sequences from time point 1 were aligned against  
731 sequences of the same gene from time point 2, once the sequences at time 2 and time 3 were determined  
732 to be the same. To determine how abundant each marker gene, and all of its variants, are at each time  
733 point, metagenome reads from each time point were mapped to its own set of marker gene sequences  
734 (BWA mem, v0.7.17, -a)<sup>42</sup>. Read counts were normalized for the length of each gene and the total number  
735 of reads sequenced per sample (RPKM)<sup>47</sup>.

736 **Acknowledgments**

737 We would like to thank the following individuals and organizations for their generosity in providing us  
738 with strains and plasmids: Tobias Dörr (STRAINS), Barth Smets (RP4), John Helmann (*B. subtilis*) and  
739 the CDC & FDA Antibiotic Resistance (AR) Isolate Bank. We would like to thank Sarah Spencer for  
740 technical advice. This study was funded by the Centers for Disease Control (OADS BAA 2016-N-17812)  
741 and by the National Sciences Foundation (Awards #1661338 and #1650122). F.N. is a SUNY Diversity  
742 Fellow. M.J.S. is funded by the NIAID (K23 AI114994). I.L.B. is funded by the NIH (1DP2HL141007-  
743 01) and is a Sloan Foundation Research Fellow, a Packard Fellowship in Science and Engineering, and a  
744 Pew Foundation Biomedical Scholar.

745 **Conflict of Interest Statement**

746 M.J.S has received grant funding from BioFire Diagnostics, Allergan, and Merck and has received  
747 consulting fees from Shionogi and Achaogen. All other authors declare that they have no conflicts of  
748 interest.

749

750 **References**

- 751 1. Sommer MO a, Dantas G, Church GM. Functional Characterization of the Antibiotic Resistance  
752 Reservoir in the Human Microflora. *Science (80- )*. 2009;325(5944):1128-1131.  
753 doi:10.1126/science.1176950
- 754 2. Kent AG, Vill AC, Shi Q, Satlin MJ, Brito IL. Widespread transfer of mobile antibiotic resistance  
755 genes within individual gut microbiomes revealed through bacterial Hi-C. doi:10.1038/s41467-  
756 020-18164-7
- 757 3. Beaulaurier J, Zhu S, Deikus G, et al. Metagenomic binning and association of plasmids with  
758 bacterial host genomes using DNA methylation. *Nat Biotechnol*. 2018;36(1):61-69.  
759 doi:10.1038/nbt.4037
- 760 4. Xu L, Brito IL, Alm EJ, Blainey PC. Virtual microfluidics for digital quantification and single-cell  
761 sequencing. *Nat Methods*. 2016;13(9). doi:10.1038/nmeth.3955
- 762 5. Lan F, Demaree B, Ahmed N, Abate AR. Single-cell genome sequencing at ultra-high-throughput  
763 with microfluidic droplet barcoding. *Nat Biotechnol*. 2017;35(7):640-646. doi:10.1038/nbt.3880
- 764 6. Zou Y, Xue W, Luo G, et al. 1,520 reference genomes from cultivated human gut bacteria enable  
765 functional microbiome analyses. *Nat Biotechnol*. 2019;37(2):179-185. doi:10.1038/s41587-018-  
766 0008-8
- 767 7. Poyet M, Groussin M, Gibbons SM, et al. A library of human gut bacterial isolates paired with  
768 longitudinal multiomics data enables mechanistic microbiome research. *Nat Med*.  
769 2019;25(9):1442-1452. doi:10.1038/s41591-019-0559-3
- 770 8. Ottesen EA, Hong JW, Quake SR, Leadbetter JR. *Microfluidic Digital PCR Enables Multigene*  
771 *Analysis of Individual Environmental Bacteria*. <http://science.sciencemag.org/>. Accessed April 9,  
772 2020.

- 773 9. Zeng Y, Novak R, Shuga J, Smith MT, Mathies RA. High-Performance Single Cell Genetic  
774 Analysis Using Microfluidic Emulsion Generator Arrays. *Proc Natl Acad Sci USA*.  
775 2008;105(4):3183-3190. doi:10.1021/ac902683t
- 776 10. Tadmor AD, Ottesen EA, Leadbetter JR, Phillips R. Probing individual environmental bacteria for  
777 viruses by using microfluidic digital PCR. 2011;333(6038):58-62.
- 778 11. Spencer SJ, Tamminen M V, Preheim SP, et al. Massively parallel sequencing of single cells by  
779 epicPCR links functional genes with phylogenetic markers SUPPLIMENT. *ISME J*.  
780 2015;(September):1-10. doi:10.1038/ismej.2015.124
- 781 12. Liu Y, Schulze-Makuch D, de Vera JP, et al. The development of an effective bacterial single-cell  
782 lysis method suitable for whole genome amplification in microfluidic platforms. *Micromachines*.  
783 2018;9(8). doi:10.3390/mi9080367
- 784 13. Tamminen M V., Virta MPJ. Single gene-based distinction of individual microbial genomes from  
785 a mixed population of microbial cells. *Front Microbiol*. 2015;6(MAR):1-10.  
786 doi:10.3389/fmicb.2015.00195
- 787 14. Finn TE, Nunez AC, Sunde M, Easterbrook-Smith SB. Serum albumin prevents protein  
788 aggregation and amyloid formation and retains chaperone-like activity in the presence of  
789 physiological ligands. *J Biol Chem*. 2012;287(25):21530-21540. doi:10.1074/jbc.M112.372961
- 790 15. Macosko EZ, Basu A, Satija R, et al. Highly parallel genome-wide expression profiling of  
791 individual cells using nanoliter droplets. *Cell*. 2015;161(5):1202-1214.  
792 doi:10.1016/j.cell.2015.05.002
- 793 16. Holmsgaard PN, Norman A, Chr S, et al. Bias in bacterial diversity as a result of Nycodenz  
794 extraction from bulk soil. *Soil Biol Biochem*. 2011;43(10):2152-2159.  
795 doi:10.1016/j.soilbio.2011.06.019



- 796 17. Hevia A, Delgado S, Margolles A, Sanchez B. Application of density gradient for the isolation of  
797 the fecal microbial stool component and the potential use thereof. *Sci Rep.* 2015;5(1):16807.  
798 doi:10.1038/srep16807
- 799 18. Vorkapic D, Pressler K, Schild S. Multifaceted roles of extracellular DNA in bacterial physiology.  
800 *Curr Genet.* 2016;62(1):71-79. doi:10.1007/s00294-015-0514-x
- 801 19. Blattner FR, Plunkett G, Bloch CA, et al. The complete genome sequence of Escherichia coli K-  
802 12. *Science (80- ).* 1997;277(5331):1453-1462. doi:10.1126/science.277.5331.1453
- 803 20. Guzman LM, Belin D, Carson MJ, Beckwith J. Tight regulation, modulation, and high-level  
804 expression by vectors containing the arabinose P(BAD) promoter. *J Bacteriol.*  
805 1995;177(14):4121-4130. doi:10.1128/jb.177.14.4121-4130.1995
- 806 21. Cantón R, González-Alba JM, Galán JC. CTX-M enzymes: Origin and diffusion. *Front Microbiol.*  
807 2012;3(APR):110. doi:10.3389/fmicb.2012.00110
- 808 22. Woerther PL, Burdet C, Chachaty E, Andremont A. Trends in human fecal carriage of extended-  
809 spectrum  $\beta$ -lactamases in the community: Toward the globalization of CTX-M. *Clin Microbiol*  
810 *Rev.* 2013;26(4):744-758. doi:10.1128/CMR.00023-13
- 811 23. Poirel L, Naas T, Nordmann P. Genetic support of extended-spectrum  $\beta$ -lactamases. *Clin*  
812 *Microbiol Infect.* 2008;14(SUPPL. 1):75-81. doi:10.1111/j.1469-0691.2007.01865.x
- 813 24. Anou M, Somboro, John Osei Sekyere, Daniel G. Amoako, Sabiha Y. Essack LAB. Diversity and  
814 Proliferation of Metallo-Beta-Lactamases: a Clarion Call for Clinically Effective Metallo-Beta-  
815 Lactamase Inhibitors. *Appl Environ Microbiol.* 2018;84(18):1-20.
- 816 25. Gerritsen J, Fuentes S, Grievink W, et al. Characterization of *Romboutsia ilealis* gen. nov., sp.  
817 nov., isolated from the gastro-intestinal tract of a rat, and proposal for the reclassification of five  
818 closely related members of the genus *Clostridium* into the genera *Romboutsia* gen. nov., *Intestinib.*

- 819 *Int J Syst Evol Microbiol.* 2014;64(Pt 5):1600-1616. doi:10.1099/ijs.0.059543-0
- 820 26. Clark RR, Judd J, Lasek-Nesselquist E, et al. Direct cell–cell contact activates SigM to express the  
821 ESX-4 secretion system in *Mycobacterium smegmatis*. *Proc Natl Acad Sci U S A.*  
822 2018;115(28):E6595-E6603. doi:10.1073/pnas.1804227115
- 823 27. Antipov D, Raiko M, Lapidus A, Pevzner PA. Plasmid detection and assembly in genomic and  
824 metagenomic data sets. *Genome Res.* 2019;29(6):961-968. doi:10.1101/gr.241299.118
- 825 28. Shkoporov AN, Hill C. Bacteriophages of the Human Gut: The “Known Unknown” of the  
826 Microbiome. *Cell Host Microbe.* 2019;25(2):195-209. doi:10.1016/j.chom.2019.01.017
- 827 29. Flores CO, Meyer JR, Valverde S, Farr L, Weitz JS. Statistical structure of host–phage  
828 interactions. *Proc Natl Acad Sci .* 2011;108(28):E288-E297. doi:10.1073/pnas.1101595108
- 829 30. Preheim SP, Olesen SW, Spencer SJ, et al. Surveys, simulation and single-cell assays relate  
830 function and phylogeny in a lake ecosystem. *Nat Microbiol.* 2016;1(9):1-9.  
831 doi:10.1038/nmicrobiol.2016.130
- 832 31. Heidelberg JF, Elsen JA, Nelson WC, et al. DNA sequence of both chromosomes of the cholera  
833 pathogen *Vibrio cholerae*. *Nature.* 2000;406(6795):477-483. doi:10.1038/35020000
- 834 32. Kunst F, Ogasawara N, Moszer I, et al. The complete genome sequence of the gram-positive  
835 bacterium *Bacillus subtilis*. *Nature.* 1997;390(6657):249-256. doi:10.1038/36786
- 836 33. Klümper U, Riber L, Dechesne A, et al. Broad host range plasmids can invade an unexpectedly  
837 diverse fraction of a soil bacterial community. *ISME J.* 2015;9(4):934-945.  
838 doi:10.1038/ismej.2014.191
- 839 34. Comai L, Howell T. Barcode Generator. 2012.  
840 [http://comailab.genomecenter.ucdavis.edu/index.php/Barcode\\_generator](http://comailab.genomecenter.ucdavis.edu/index.php/Barcode_generator).

- 841 35. Alcock BP, Raphenya AR, Lau TTY, et al. CARD 2020: Antibiotic resistome surveillance with  
842 the comprehensive antibiotic resistance database. *Nucleic Acids Res.* 2020;48(D1):D517-D525.  
843 doi:10.1093/nar/gkz935
- 844 36. Edgar RC. Search and clustering orders of magnitude faster than BLAST. *Bioinformatics.*  
845 2010;26(19):2460-2461. doi:10.1093/bioinformatics/btq461
- 846 37. Caporaso JG, Kuczynski J, Stombaugh J, et al. QIIME allows analysis of high-throughput  
847 community sequencing data. *Nat Methods.* 2010;7(5):335-336. doi:10.1038/nmeth.f.303
- 848 38. Martin M. Cutadapt removes adapter sequences from high-throughput sequencing reads.  
849 *EMBnet.journal.* 2011;17(1):10. doi:10.14806/ej.17.1.200
- 850 39. Schloss PD, Westcott SL, Ryabin T, et al. Introducing mothur: Open-source, platform-  
851 independent, community-supported software for describing and comparing microbial  
852 communities. *Appl Environ Microbiol.* 2009;75(23):7537-7541. doi:10.1128/AEM.01541-09
- 853 40. Quast C, Pruesse E, Yilmaz P, et al. The SILVA ribosomal RNA gene database project: Improved  
854 data processing and web-based tools. *Nucleic Acids Res.* 2013;41(D1):D590.  
855 doi:10.1093/nar/gks1219
- 856 41. Camacho C, Coulouris G, Avagyan V, et al. BLAST+: architecture and applications. *BMC*  
857 *Bioinformatics.* 2009;10(1):421. doi:10.1186/1471-2105-10-421
- 858 42. Li H. *Aligning Sequence Reads, Clone Sequences and Assembly Contigs with BWA-MEM.*; 2013.
- 859 43. Nurk S, Bankevich A, Antipov D, et al. Assembling Single-Cell Genomes and Mini-Metagenomes  
860 From Chimeric MDA Products. *J Comput Biol.* 2013;20(10):714-737. doi:10.1089/cmb.2013.0084
- 861 44. Wu M, Scott AJ. Phylogenomic analysis of bacterial and archaeal sequences with AMPHORA2.  
862 *Bioinformatics.* 2012;28(7):1033-1034. doi:10.1093/bioinformatics/bts079

- 863 45. Buchfink B, Xie C, Huson DH. Fast and sensitive protein alignment using DIAMOND. *Nat*  
864 *Methods*. 2015;12(1):59-60. doi:10.1038/nmeth.3176
- 865 46. Altschul SF, Gish W, Miller W, Myers EW, Lipman DJ. Basic local alignment search tool. *J Mol*  
866 *Biol*. 1990;215(3):403-410. doi:10.1016/S0022-2836(05)80360-2
- 867 47. Mortazavi A, Williams BA, McCue K, Schaeffer L, Wold B. Mapping and quantifying  
868 mammalian transcriptomes by RNA-Seq. *Nat Methods*. 2008;5(7):621-628.  
869 doi:10.1038/nmeth.1226
- 870